ASN NEURO RESEARCH ARTICLE

ASN NEURO 2(2):art:e00030.doi:10.1042/AN20090048

Hyperglycaemia and diabetes impair gap junctional communication among astrocytes

Gautam K Gandhi*, Kelly K Ball†, Nancy F Cruz† and Gerald A Dienel*,†1

*Department of Physiology and Biophysics, University of Arkansas for Medical Sciences, Little Rock, AR 72205, U.S.A.

†Department of Neurology, University of Arkansas for Medical Sciences, Little Rock, AR 72205, U.S.A.

Cite this article as: Gandhi GK, Ball KK, Cruz NF and Dienel GA (2009) Hyperglycaemia and diabetes impair gap junctional communication among astrocytes. ASN NEURO 2(2):art:e00030.doi:10.1042/AN20090048

ABSTRACT

Sensory and cognitive impairments have been documented in diabetic humans and animals, but the pathophysiology of diabetes in the central nervous system is poorly understood. Because a high glucose level disrupts gap junctional communication in various cell types and astrocytes are extensively coupled by gap junctions to form large syncytia, the influence of experimental diabetes on gap junction channel-mediated dye transfer was assessed in astrocytes in tissue culture and in brain slices from diabetic rats. Astrocytes grown in 15–25 mmol/l glucose had a slow-onset, poorly reversible decrement in gap junctional communication compared with those grown in 5.5 mmol/l glucose. Astrocytes in brain slices from adult STZ (streptozotocin)-treated rats at 20–24 weeks after the onset of diabetes also exhibited reduced dye transfer. In cultured astrocytes grown in high glucose, increased oxidative stress preceded the decrement in dye transfer by several days, and gap junctional impairment was prevented, but not rescued, after its manifestation by compounds that can block or reduce oxidative stress. In sharp contrast with these findings, chaperone molecules known to facilitate protein folding could prevent and rescue gap junctional impairment, even in the presence of elevated glucose level and oxidative stress. Immunostaining of Cx (connexin) 43 and 30, but not Cx26, was altered by growth in high glucose. Disruption of astrocytic trafficking of metabolites and signalling molecules may alter interactions among astrocytes, neurons and endothelial cells and contribute to changes in brain function in diabetes. Involvement of the microvasculature may contribute to diabetic complications in the brain, the cardiovascular system and other organs.

Key words: astrocyte, connexin (Cx), diabetes, gap junction, hyperglycaemia, streptozotocin.

INTRODUCTION

Many diverse, progressive and severe complications of diabetes are well established and are linked to chronically high glucose levels in conjunction with insulin deficiency (Type 1 diabetes) or insulin resistance (Type 2 diabetes). The complex, multifactorial pathobiology of diabetes (Brownlee, 2005) includes non-specific glycation reactions of glucose, increased sorbitol production and osmotic stress, oxidative stress due to generation of ROS (reactive oxygen species)/RNS (reactive nitrogen species), depletion of endogenous anti-oxidants, enhanced lipid peroxidation, metabolic changes, altered hormonal responses, cardiovascular disease, kidney damage, poor wound healing, and cataract formation. Overall, the impact of diabetes on the central nervous system is generally considered to be mild or modest compared with involvement of peripheral organs and peripheral neuropathies (Little et al., 2007), which have severe consequences for both the quality and duration of life of diabetic patients.

Diabetes does, however, affect the brain, altering blood flow, blood–brain barrier integrity, brain metabolism and neurotransmitters, and cognitive function in diabetic patients and in animal models, but these findings are sometimes contradictory due, in part, to differences in duration, severity and control of the disease and to methodological issues (McCall, 1992, 2004, 2005; Mooradian, 1997; Allen et al., 2004; Sima et al., 2004; Biessels and Gispen, 2005; Huber et al., 2006; Kamal et al., 2006; Brands et al., 2007; DCCT/EDIC, 2007; Kodl and Seaquist, 2008; Manschot et al., 2008; Roberts

[1] To whom correspondence should be addressed (email gadienel@uams.edu).

Abbreviations: aCSF, artificial cerebrospinal fluid; Cx, connexin; DCF, 2′,7′-dichlorodihydrofluorescein; carboxy-DCF-DA, carboxy DCF diacetate; dBcAMP, dibutyryl cAMP; DIC, differential interference contrast; DMEM, Dulbecco's modified Eagle's medium; ER, endoplasmic reticulum; FBS, fetal bovine serum; L-NAME, L-N^{ω}-nitro-L-arginine methyl ester; LYCH, Lucifer Yellow CH; LYVS, Lucifer Yellow VS; MnTBAP, manganese(III) tetrakis (4-benzoic acid) porphyrin chloride; NA, numerical aperture; 6-NBDG, 6-[*N*-(7-nitrobenz-2-oxa-1,3-diazol-4-yl)amino]-2-deoxyglucose; NOS, nitric oxide synthase; 4-PBA, 4-phenylbutyric acid; PKC, protein kinase C; RNS, reactive nitrogen species; ROS, reactive oxygen species; STZ, streptozotocin; TMAO, trimethylamine N-oxide dihydrate; TUDCA, tauroursodeoxycholic acid.

et al., 2008). Specific brain functions are measurably impaired in diabetic patients, including increased latencies of visual and auditory evoked potentials (Buller et al., 1988; Di Mario et al., 1995; Díaz de León-Morales et al., 2005) and hearing deficits (Tay et al., 1995; Frisina et al., 2006; Vaughan et al., 2006, 2007), all with unidentified aetiologies. Alloxan- and STZ (streptozotocin)-treated diabetic rats have abnormal visual and auditory evoked potentials (Buller et al., 1986; Rubini et al., 1992; Biessels et al., 1999; Manschot et al., 2003), impaired long-term potentiation and facilitated long-term depression in hippocampal neurons, and abnormal water maze learning skills (Biessels et al., 1998, Kamal et al., 1999, 2006; Biessels et al., 2005). Together, these findings suggest that subtle or sub-clinical functional disturbances in diabetic brain may be more widespread than generally recognized and may affect auditory, visual and other sensory processing pathways, as well as cognitive capability.

Our interest in the involvement of astrocytes in diabetic complications of the central nervous system arose from reports of impaired gap junctional communication in hyperglycaemic vascular smooth muscle, endothelial cells and retinal pericytes (Inoguchi et al., 1995; Stalmans and Himpens, 1997; Kuroki et al., 1998; Oku et al., 2001; Sato et al., 2002; Li et al., 2003). We recently found that astrocytes in the inferior colliculus, an auditory pathway structure with the highest metabolic rate in brain, are highly coupled by gap junctions (Ball et al., 2007) and are involved in selective syncytial 'trafficking' of energy and redox metabolites (Gandhi et al., 2009a), including lactate (Gandhi et al., 2009b). (Note: in the present study, metabolite 'trafficking' refers to transfer among cells of small molecules involved in metabolism, energetics and signalling by processes driven mainly by concentration gradients. Trafficking of small molecules involves diffusion and transporters, and differs from protein 'trafficking'. Fluorescent dyes are used as surrogate markers to visualize and quantify movements of small molecules among cells.) We hypothesized that diabetes may cause 'silent' changes affecting astrocytic communication and metabolite trafficking via gap junctions may alter interactions among astrocytes, neurons and endothelial cells (i.e. the neurovascular unit), thereby contributing to the slow, progressive brain dysfunction in diabetes. The present study, therefore, examined the effects of experimental diabetes on astrocytic gap junctional transport using two model systems, the STZ-diabetic rat and cultured astrocytes grown in medium containing very high glucose concentrations.

Studies in rat models of diabetes show that plasma and brain glucose levels increase on average by approx. 3-fold, with mean values in brain rising from 2.2 μmol/g in controls to 6.9 μmol/g in diabetic animals (Table 1). In STZ-diabetic rats, the increases in plasma and brain glucose content occur within 2 days after STZ treatment and persist for months at levels similar to those in spontaneously diabetic rats (Table 1). The rise in brain glucose concentration with an increase in plasma glucose level is the expected consequence of concentration gradient-driven transport of glucose across the blood–brain barrier. Under steady state conditions in normal rats infused with various concentrations of glucose, the brain glucose level is approx. 20% that in plasma in the normo- and hyper-glycaemic range; in contrast, the brain plasma glucose distribution ratio falls during hypoglycaemia when glucose supply does not match demand (Dienel et al., 1991, 1997; Holden et al., 1991). Thus brain glucose level rises when plasma glucose concentration increases, and in diabetic rats the brain: plasma glucose distribution ratio is even higher, approx. 50% greater than in control rats, and the elevated ratio is not normalized by acute insulin treatment to reduce plasma glucose level to the normal range (Hofer and Lanier, 1991a, 1991b). Corresponding studies of brain glucose level in human diabetics are sparse, but one NMR study reported a 1.5-fold increase in the level of glucose relative to creatine in diabetic brain and calculated a net rise in brain glucose level of approx. 2 mmol/l (Table 1). Routine commercially available tissue culture media contain glucose concentrations as high as 25 mmol/l glucose, which approximates to the level of glucose in the plasma of diabetic animals and exceeds the normal and diabetic rat brain glucose level by approx. 10- and 3-fold respectively (Table 1). Astrocytes grown in 'high'-glucose media would be exposed to the myriad of well-established consequences of severe, chronic hyperglycaemia, and the pathophysiological consequences of neuronal and Schwann cell culture in high-glucose media have been recently emphasized by Kleman et al. (2008) and Mîinea et al. (2002). In the present study, astrocytes chronically exposed to elevated glucose levels *in vivo* and *in vitro* were used as models of experimental diabetes. We report that intercellular gap junction-mediated communication among astrocytes is markedly reduced in cultured cerebral cortical astrocytes and in slices of inferior colliculus from STZ-treated rats, and that pharmacological intervention can protect against or restore this impairment.

MATERIALS AND METHODS

Reagents

DMEM (Dulbecco's modified Eagle's medium; low glucose, catalogue no. 12320-032, and high glucose, no. 12430-054), penicillin, streptomycin, amphotericin B and trypsin were obtained from Invitrogen (Carlsbad, CA, U.S.A.). FBS (fetal bovine serum) was purchased from Hyclone (Logan, UT, U.S.A.). dBcAMP (dibutyryl cAMP), L-LME (L-leucine methyl ester hydrochloride), octanol, cytochalasin B, LYVS (Lucifer Yellow VS, dilithium salt), LYCH (Lucifer Yellow CH, dilithium salt), L-NAME (N^{ω}-nitro-L-arginine methyl ester), 4-PBA (4-phenylbutyric acid), glycerol, butyric acid and *N*-(methyl-nitrosocarbamoyl)-α-D-glucosamine (STZ) were from Sigma–Aldrich (St Louis, MO, U.S.A.). Rhodamine–dextran, 6-NBDG {6-[*N*-(7-nitrobenz-2-oxa-1,3-diazol-4-yl)amino]-2-deoxy-glucose}, Alexa Fluor® 350 carboxylic acid, succinimidyl ester

Table 1 **Plasma and brain glucose concentrations in experimental diabetes**

BB/Wor, BioBredding/Worcester; Cr, creatine; Glc, glucose; STZ, streptozotocin.

(a)

	Arterial plasma glucose (μmol/ml)			Brain glucose (μmol/g)			
Rat/duration/treatment	Control	Diabetic	Diabetic/control	Control	Diabetic	Diabetic/control	Reference
2 Days/STZ	7.7*	27.7*	3.6	1.8	6.5	3.6	Folbergrová et al. (1992)
2–3 days/STZ	10.5*	28*	2.7	2.9	11.4	3.9	Ruderman et al. (1974)
3 day/STZ	16.9	30.9	1.8	2.4 (CSF=7.3 mmol/ml)	8.7 (CSF= 12.9 mmol/ml)	3.6 (CSF=1.8 mmol/ml)	Shram et al. (1997)
1 week/STZ	8.2	25.0	3.0	2.1	8.1	3.9	Hofer and Lanier (1991a)
1 week/STZ	8.6	25.9	3.0	3.2	12.2	3.8	Lanier et al (1996)
1 or 4 weeks/STZ	7.4†	30.0† (1 week); 16.3† (4 weeks)	4.1	2.4	6.2 (1 and 4 weeks)	2.6	Mans et al. (1988)
10 days/STZ	10.4	26	2.5	2.3	4.5	2.0	García-Espinosa et al. (2003)
12 day/STZ; given insulin for 8 days; assayed 4 days after insulin withdrawal	7.6*	28*	3.7	1.7	6.6	3.9	Blackshear and Alberti (1974)
2 weeks/STZ	9.4	24.7	2.6	1.2‡	2.2‡	1.8	Hoxworth et al. (1999)
2 weeks/STZ	5.4	22.7	4.2	2.4	9.5	3.9	Wagner and Lanier (1994)
6–8 weeks/STZ	11.3*	26.9*	2.4	~2.3‡	~3.7‡ (not statistically significant)	1.6	Tang et al. (2000)
12 weeks/STZ	12.5	24.4	2.0	2.3‡	3.7‡	1.6	Puchowicz et al. (2004)
Spontaneously diabetic Wistar rat	7.6	23.6	3.1	1.7	7.6	4.5	Hofer and Lanier (1991b)
20–28 weeks/ spontaneously diabetic Zucker rat,	8.4*†	38.9*†	4.6	1.7	4.9	2.9	van der Graaf et al. (2004)
BB/Wor diabetic Sprague–Dawley rat	8	22	2.8	2.1§	7.5§	3.6	Jacob et al. (2002)
Mean ± S.D. (n=15)	9.3 ± 2.8	27.0 ± 4.2 (P<0.001)	3.1 ± 0.8	2.2 ± 0.5	6.9 ± 2.8 (P<0.001)	3.1 ± 1.0	

(b)

	Arterial plasma glucose (μmol/ml)			Relative value (Glc/Cr)			
Human	Control	Diabetic	Diabetic/control	Control	Diabetic	Diabetic/control	Reference
Values	5.6–8.4*	13.9*	1.7–2.5	0.13||/0.12||	0.21||/0.18||	1.62 (parietal cortex)/ 1.50 (occipital cortex)	Kreis and Ross (1992)

* Calculated from reported glucose level in whole blood by multiplying by the plasma/blood concentration ratio for glucose of 1.4 (Heath and Rose, 1969).
† Blood drawn from inferior vena cava or tail vein.
‡ Calculated from reported values of nmol/mg dry weight, assuming 1 mg dry weight/10 mg wet weight.
§ Values measured in microdialysate of extracellular fluid in the inferior colliculus.
|| NMR assays of glucose level relative to creatine in cerebral cortex; the authors calculated that the excess glucose level in diabetic brain was approx. 2 mmol/l.

(A350), carboxy-DCF-DA [carboxy DCF (2′,7′-dichlorodihydrofluorescein) diacetate] and DCF-DA were from Invitrogen (Molecular Probes, Eugene, OR, U.S.A.). TMAO (trimethylamine N-oxide dihydrate) was from Acros Organics (Fisher Scientific, Pittsburgh, PA, U.S.A.); TUDCA (tauroursodeoxycholic acid, sodium salt), tunicamycin (*Streptomyces lysosuperficus*) and MnTBAP [manganese(III) tetrakis(4-benzoic acid) porphyrin chloride] were from Calbiochem (EMD Biosciences, La Jolla, CA, U.S.A.). Affinity-purified rabbit polyclonal antibodies against Cx43 (catalogue number 71-0700), Cx30 (71-2200) and Cx26 (51-2800) and the goat anti-rabbit Texas Red-labelled secondary antibody were from Invitrogen; goat serum was from Dako (Carpinteria, CA, U.S.A.).

Astrocyte culture

Cultured astrocytes were prepared by small modifications of established procedures (Hertz et al., 1998). Briefly, astrocytes were harvested from the cerebral cortex of 1-day-old albino Wistar–Hanover rats (Taconic Farms, Germantown, NY, U.S.A.)

and grown in T-75 culture flasks with DMEM containing 5.5 mmol/l glucose, 10% (v/v) FBS, 50 IU (international units) of penicillin and 50 μg/ml of streptomycin at 37°C in humidified air containing 5% CO_2. L-LME (0.1 mmol/l), a lysosomotrophic agent that selectively destroys mononuclear cells including microglia, was also included in the culture medium, and the cultures were shaken by hand twice per week to remove microglia. When confluent, the cells were trypsinized, seeded on to polylysine-coated glass coverslips and grown to confluence in a medium containing amphotericin B (2.5 μg/ml). Then differentiation was induced by supplementing the culture medium with 0.25 mmol/l dBcAMP. The next day, cells were maintained in a medium containing 0.25 mmol/l dBcAMP and 5.5, 15 or 25 mmol/l glucose for up to 4 weeks. Purity of cultures was based on the expression of the astrocyte marker, glial fibrillary acidic protein, which was expressed in >90% of the cells.

STZ-induced diabetes

Male Sprague–Dawley rats (200–300 g; Harlan, Indianapolis, IN, U.S.A.) were fasted overnight, injected intraperitoneally with STZ (65 mg/kg body weight in 33 mmol/l citrate-buffered saline, pH 4.5); controls received the same volume of citrate-buffered saline (Romanovsky et al., 2006). Tail blood samples were taken for glucose determination from overnight-fasted animals on the day before STZ injection and on days 3, 8 and 13 thereafter; rats were categorized as normoglycaemic or hyperglycaemic, using a cut-off value of >6.9 mmol/l to define hyperglycaemia based on the day 3 fasting blood glucose level. All animal use procedures were in strict accordance with the NIH Guide for Care and Use of Laboratory Animals and were approved by the local Animal Care and Use Committee.

Brain slice preparation

At 20–24 weeks after induction of STZ-diabetes, the diabetic and age-matched, vehicle-injected control rats were deeply anaesthetized with halothane and decapitated and their brains were quickly removed and chilled by immersion in an oxygenated (i.e. bubbled with O_2/CO_2, 95:5), ice-cold aCSF (artificial cerebrospinal fluid) solution (concentrations in mmol/l: 26 $NaHCO_3$, 10 glucose, 124 NaCl, 2.8 KCl, 2.0 $MgSO_4$, 1.25 NaH_2PO_4 and 2.0 $CaCl_2$, pH 7.3) and 248 sucrose, and 250 μm-thick slices were cut using a Leica (Heidelberg, Germany) VT 1000S tissue slicer; inferior colliculus slices were incubated in oxygenated aCSF containing sucrose for 30 min at 35°C and then for 1 h at 22°C (Moyer and Brown, 1998). Slices of inferior colliculus were transferred to an open bath perfusion chamber (Warner Instruments, Hamden, CT, U.S.A.) on the microscope stage. Then the slices of inferior colliculus and the cultured astrocytes were perfused (1 ml/min) with aCSF that was continuously bubbled with O_2/CO_2 (95:5) and contained 26 mmol/l $NaHCO_3$ (pH 7.3) and 10 mmol/l glucose at approx. 21–22°C.

Gap junction dye transfer assays

Two procedures were used to insert a membrane-impermeant dye into astrocytes to assay gap junctional communication, scrape-loading (el-Fouly et al., 1987; Giaume et al., 1991) and diffusion into a single cell impaled with a micropipette (Ball et al., 2007; Gandhi et al., 2009a). Scrape loading is commonly used for dye transfer assays because it is a simple procedure, but the procedure destroys cells at the scrape site and releases their contents to the medium; it requires medium changes and washing of cells after dye loading, and it cannot be used in tissue slices in which astrocytes have formed their syncytia during normal brain development involving interactions of astrocytes with neurons and the vasculature. Microinjection of cells is technically more difficult, but offers more control for dye loading, and it can be used in brain slices. Fluorescent compounds used to assay dye transfer were LYVS (4% or 62 mmol/l), 4% LYVS plus 4% LYCH, Alexa Fluor® 350 (5 mmol/l) and 6-NBDG (20 mmol/l). 6-NBDG is a non-metabolizable fluorescent analogue of glucose that is a substrate for glucose transporters. In the brain slice assays of 6-NBDG gap junctional transfer, 10 μmol/l of cytochalasin B, a glucose transport inhibitor (Speizer et al. 1985), was included to minimize efflux of 6-NBDG from cells via glucose transporters. In these assays, an excess amount of pyruvate (10 mmol/l) was added to the perfusate as an oxidative fuel to compensate for blockade of glucose transport.

Scrape loading

The procedure of Giaume et al. (1991) was used for scrape-load assays, as follows. Glass coverslips containing astrocytes were transferred to sterile 35 mm culture dishes; coverslips were washed once and incubated in ionic-buffered solution containing (concentrations in mmol/l) 130 NaCl, 2.8 KCl, 1 $CaCl_2$, 2 $MgCl_2$ and 10 Hepes (pH 7.2) for 1 min, washed again and incubated in calcium-free medium for 1 min. The medium was replaced with a calcium-free medium containing 0.5 mg/ml LYVS and 1 mmol/l rhodamine–dextran (a non-permeant macromolecule used to label the scrape-loaded cells); a 2–3 cm scrape was made with a razor blade, and dye transfer was allowed for 2 min. Giaume et al. (1991) stated that calcium was omitted from the medium during scrape-loading because 1 mmol/l Ca^{2+} blocks Lucifer Yellow transfer; Mg^{2+} was still included in the scrape-load medium. A recent study showed that incubation of cultured astrocytes in the nominal absence of extracellular bivalent cations (Ca^{2+} and Mg^{2+}) opens channels (hemichannels or pannexin channels) that allow rapid, widespread entry of Lucifer Yellow into astrocytes (Ye et al., 2003); the presence of Mg^{2+} during the scrape-loading would prevent opening of these channels. Cells were washed twice with calcium containing ionic-buffered solution and dye-labelled area determined at 8 min after scraping by image analysis using MetaVue software. Line scans were used to evaluate the change in Lucifer Yellow fluorescent intensity as a function of distance from the scrape site. The

dye-labelled area was determined in three regions of each scrape; regions were imaged, and gap junctional dye transfer was calculated as the difference between the areas labelled by LYVS (gap junction permeable) and rhodamine–dextran (labels the dye-loaded cells); the mean value for each triplicate determination was used as the area labelled in that scrape-load assay.

Dye diffusion into single cells

For single-cell dye loading with micropipettes, cultured astrocytes were visualized under DIC (differential interference contrast) and astrocytes in brain slices were visualized under IR-DIC (IR-differential interference contrast) (Dodt and Zieglgänsberger, 1990) using a Nikon Eclipse E600 microscope (Nikon, Melville, NY, U.S.A.) equipped with a Nikon Fluor $\times 40$ [NA (numerical aperture)$=0.80$] objective and Photometrics CoolSNAP ES camera (Roper Scientific, Atlanta, GA, U.S.A.). Micropipettes with 12–14 MΩ resistance (tip inner diameter: 1.0 ± 0.1 μm, outer diameter: 1.8 ± 0.1 μm; means $\pm$ S.D.) were constructed from borosilicate glass (1 mm outer diameter, 0.5 mm inner diameter) using a P97 pipette puller (Sutter Instruments, Novato, CA, U.S.A.) and filled with a test solution containing a fluorescent probe. Except where noted, micropipette solutions contained (composition in mmol/l) 21.4 KCl, 0.5 $CaCl_2$, 2 $MgCl_2$, 5 EGTA, 2 ATP, 0.5 GTP, 2 ascorbate and 10 Hepes, pH 7.2, and one of three fluorescent dyes (LYVS, excitation/emission maxima: 430/530 nm; 6-NBDG, 475/550 nm; or Alexa Fluor® 350, 346/442 nm). The osmolarity of each solution was measured (Osmette II; Precision Systems, Natick, MA, U.S.A.) and adjusted to 305–320 mOsm/l with sucrose. Astrocytes were impaled with micropipettes using an MP-225 manipulator (Sutter Instruments, San Francisco, CA, U.S.A.), and tracers were diffused into cells for 2 min in cultured cells and for 5 min in brain slices. Fluorescence intensity was determined using MetaVue software before (background) and after diffusion of the test compound into a single astrocyte, and the dye-labelled area was determined with MetaVue software (Ball et al., 2007; Gandhi et al., 2009a). In brain slice assays, cells labelled with LYVS were counted after cutting the 250 μm-thick slices into 10 μm-thick serial sections; the number of labelled cells was based on counts of the prominently labelled nuclei. The area labelled by 6-NBDG in slices was measured in the intact slice with MetaVue software. Gap junctional transfer was inhibited by pretreatment with octanol (final concentration, 0.6 mmol/l).

Dye transfer was also assayed in astrocytes cultured in media containing 5.5 or 25 mmol/l glucose for up to 21 days in the presence or absence of compounds to reduce ROS/RNS levels or that facilitate protein folding. MnTBAP (50 μmol/l) is a superoxide dimutase mimetic that is a scavenger of ROS (Kowluru and Abbas, 2003) and L-NAME (1 mmol/l), a competitive inhibitor of NOS (nitric oxide synthase) that impairs formation of nitric oxide and RNS (Hink et al., 2001). Chemical chaperones (Brown et al., 1996; Welch and Brown, 1996; Özcan et al., 2006), 4-PBA (1 mmol/l), glycerol (25 mmol/l), TUDCA (25 mmol/l) and TMAO (100 mmol/l) were added to the culture media at the time intervals indicated. Tunicamycin (100 ng/ml, 16 h), an inhibitor of N-linked glycosylation that causes ER (endoplasmic reticulum) stress, served as the positive control for ER stress; butyrate (1 mmol/l) was a control for 4-PBA. After cultured astrocytes were treated for the time intervals indicated, LYVS transfer was assayed by impaling a single astrocyte with a micropipette, allowing the dye to diffuse for 2 min, and then the dye-labelled area was measured using MetaVue software.

Oxidative stress assays

Astrocytes were grown in 5.5 or 25 mmol/l glucose in the presence or absence of inhibitors or chaperones, and 'oxidative stress' was assayed with DCF-DA or carboxy-DCF-DA, compounds that are cell membrane permeable, cleaved by intracellular esterases and, after oxidation by various reactive compounds, become fluorescent dichlorofluorescein (DCF) or carboxy-DCF (Tampo et al., 2003; Cruthirds et al., 2005 and references cited in these studies). At indicated days in culture, DCF-DA (10 μmol/l) was added to the culture medium (that had been changed 24 h earlier) or to a fresh medium containing the inhibitors plus 30 μmol/l DCF-DA. Cells were returned to the CO_2 incubator for 30 min at 37°C, then washed with perfusion solution, and DCF fluorescence intensity was measured with the Nikon E600 microscope ($\times 40$ objective) and MetaVue software. Ten field-of-view images were collected per coverslip, and analysed by thresholding to include the pixels with the highest 30% or highest 2% fluorescence intensity; the 30% threshold value excluded background fluorescence and included the cell bodies plus 'hot spots', whereas the 2% threshold included only the highest-intensity 'hot spots'. Slices of inferior colliculus from diabetic rats were incubated for 30 min in 10 μmol/l carboxy-DCF-DA and fluorescence intensity assayed as described above.

Cx immunostaining

Cultured astrocytes on coverslips were fixed with 2% (w/v) paraformaldehyde in 0.1 M PBS for 10 min, washed three times with PTX (0.1 M PBS containing 0.3% Triton X), blocked in 10% (v/v) goat serum in PTX for 30 min, and incubated with rabbit polyclonal primary antibodies (diluted in 10% goat serum in PTX as follows: Cx43, 1:250 to a final concentration of 1 μg/ml; Cx30, 1:250, to 1 μg/ml; Cx26, 1:25, to 5 μg/ml) for 2 h at room temperature (approx. 21–22°C) and then overnight at 4°C. The manufacturer's recommended levels for use in frozen sections were 1–5 μg/ml for Cx43 and Cx30 antibodies and 10–20 μg/ml for Cx26; in the present study, the dilution of Cx43 was the same as that used by Ye et al. (2003). The next day, samples were warmed to room temperature, washed with PTX (three 5 min washes), incubated with goat anti-rabbit secondary antibod-

ies conjugated to Texas Red (diluted 1:500 in 10% goat serum in PTX) for 1 h at room temperature, given three 5-min washes with PTX and stored at 4°C in PBS. Immunostained Cx protein includes intracellular punctate or vesicle-like structures (probably ER, Golgi apparatus and cytoplasmic vesicles; see Wolff et al., 1998 and references cited therein), that were prominent in the images of immunoreactive Cxs under the fixation and immunoassay conditions used in the present study (see the Results section). The area of this punctate or vesicular immunoreactive material was measured by image analysis of composite images of z-stacks using the maximum projection setting with a Nikon E600 microscope with confocal attachments and a ×60 water immersion objective (NA 1.00) and MetaVue software. The minimal fluorescence intensity threshold value was set to only include prominent punctate or vesicle-like structures, and integrated morphometric analysis was used to measure their total area in each of the 16–36 cells per Cx group that were derived from two independent cultures.

Statistics

Comparisons between two groups of independent samples were made with two-tailed, unpaired *t* tests. Comparisons among three or more groups of independent samples were made with one-way ANOVA and Dunnett's test for multiple comparisons against the same control value or the Bonferroni test for multiple comparisons among experimental groups. $P<0.05$ was considered to be statistically significant. All statistical analyses were performed with GraphPad Prism® software, version 5.02 (GraphPad Software, La Jolla, CA, U.S.A.).

RESULTS

Severe hyperglycaemia reduces dye transfer through gap junctional channels

Transcellular spreading LYVS after scrape-loading of astrocytes grown for 3 weeks in 5.5 mmol/l glucose greatly exceeded that of astrocytes grown in 25 mmol/l glucose (Figure 1A). Line scan analysis of Lucifer Yellow fluorescence intensity with distance showed that overall LYVS fluorescence level was higher and dye spread extended further from the scrape site in cells grown in the lower glucose concentration (Figure 1B). The mean LYVS intensity in the pixels closest to the scrape site (at 0.6 μm) tended to be higher ($P=0.084$) in the low-glucose cultures and it reached a peak (~2600 fluorescence units) at 26–29 μm from the scrape, whereas the high-glucose cultures had a much lower mean maximal value (~1700 fluorescence units; $P<0.001$) and a broader peak that was closer (7.7–20 μm) to the scrape (Figure 1B). At 90–100 μm from the scrape the fluorescence intensities in the low glucose group were still

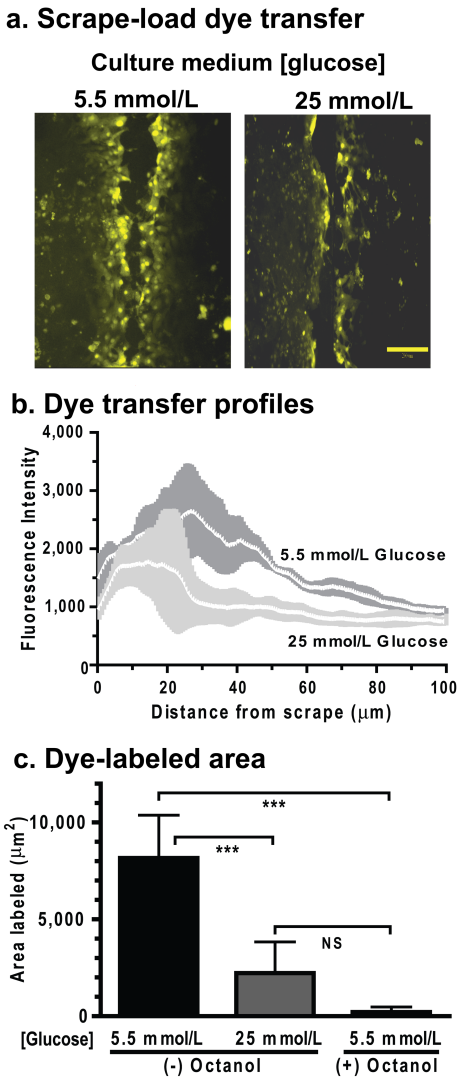

Figure 1 Growth of astrocytes in high glucose reduces gap junctional communication

(**A**) Cultured astrocytes were grown in low or high glucose for 21 days, and gap junctional transfer of LYVS (1 mmol/l) was assayed by dye transfer after scrape loading. The scrapes are in the centre of each panel, and the scale bar (100 μm) applies to both panels. (**B**) Line scan analysis (using a 100 μm bar and MetaVue software) of Lucifer Yellow fluorescence as a function of distance from the scrape; the white lines are the means for three assays and shaded areas represent ±1 S.D. (**C**) Dye-labelled area assayed in the absence ($n=15$ for 5.5 mmol/l glucose; $n=9$ for 25 mmol/l glucose) or presence ($n=4$) of octanol (final concentration 0.6 mmol/l, 10 min) to block gap junctions; values are means and vertical bars are 1 S.D. The Lucifer Yellow-labelled area was calculated as the difference in areas labelled by Lucifer Yellow and rhodamine–dextran (1 mmol/l), a gap junction-impermeant tracer that labels only the scrape-loaded cells. ***$P<0.001$; NS, not significantly different; ANOVA and the Bonferroni test.

22% higher ($P<0.001$) than in the higher glucose group. These findings suggest that the lower dye levels and reduced dye spread in severely hyperglycaemic astrocytes are not due to differential release of Lucifer Yellow from cells during the scrape load procedure via Cx 'hemichannels' or pannexin channels. If these channels were preferentially open to the medium in either group of cells, extensive dye labelling would

be expected to increase markedly throughout the culture, not just adjacent to the scrape site, as observed (Figures 1A and 1B); this labelling would be readily detected by visual observation because the LYVS causes prominent labelling of nuclei.

The net area labelled by LYVS was calculated by subtracting the area of the scrape-filled cells (i.e. area labelled by the gap junction-impermeant tracer, rhodamine–dextran) from that labelled by LYVS. Astrocytes grown in low glucose had a 4-fold higher dye-labelled area than those grown in high glucose (Figure 1C). Blockade of gap junctions with octanol reduced the LYVS-labelled area (Figure 1C) to the level of that labelled by rhodamine–dextran (results not shown).

Prolonged exposure to high glucose is required to reduce dye transfer

Glucose concentration in the culture medium did not affect astrocyte viability, and astrocytes grown in 5.5, 15 and 25 mmol/l glucose had similar cell densities on days 3, 14 and 21 (results not shown), as illustrated in Figure 2 for representative cultures grown for 2 weeks in 5.5 mmol/l (Figure 2A) or 25 mmol/l (Figure 2B) glucose. However, when gap junctional communication was assayed by impaling a single astrocyte with a micropipette and diffusing Lucifer Yellow into one cell, dye spreading from the impaled cell was much greater in cells grown for 3 weeks in 5.5 mmol/l glucose (Figure 2C) compared with those grown in 25 mmol/l glucose (Figure 2D), confirming the results of scrape-load assays (Figure 1).

Time in culture did not affect the area labelled by Lucifer Yellow in astrocytes grown in low glucose, but those grown in high glucose had a progressive decrease in gap junctional communication (Figure 2E). Impaired LYVS transfer had a slow onset, requiring approx. 3–5 days exposure to 15 or 25 mmol/l glucose before a statistically significant decrement was detectable. The time courses and maximal inhibition for cells grown in 15 and 25 mmol/l glucose were similar; the maximal decrement in gap junctional communication was relatively stable at approx. 50% of that in the low-glucose cultures during the interval from 7 to 21 days (Figure 2E).

Diffusion of a smaller fluorescent dye, Alexa Fluor® 350, among astrocytes was stable with time in the low-glucose cultures, and it also exhibited a progressive fall in labelled area in the high-glucose cultures (Figure 2F). There was a 5-day delay before Alexa Fluor® 350-labelled area was reduced by high glucose, and the 50% decrement was stable between 7 and 21 days. Thus the two dyes had similar lag times, temporal profiles and maximal reduction of labelled area, suggesting that reduced dye transfer may not be simply due to partial constriction of the gap junctional channel to block the passage of larger molecules (Alexa Fluor® 350 has a molecular mass of 311 Da after hydrolysis of the succinimidyl ester by water compared with 536 Da for the ionized form of LYVS). Note that Alexa Fluor® 350 does label a greater area than the LYVS in the low-glucose cultures (e.g. $P<0.01$ on day 1; compare Figures 2E and 2F); this is probably due mainly to its high fluorescence quantum yield (the concentration of Alexa Fluor® 350 in the micropipette was 5 mmol/l compared with 62 mmol/l for LYVS), and perhaps also to its smaller size.

Dye transfer deficit is not restored by subsequent glycaemic control

When astrocytes were grown in 15 or 25 mmol/l glucose for 2 weeks and then transferred to 5.5 mmol/l glucose for an additional 2 weeks, LYVS spreading via gap junctions did not recover. Dye transfer remained subnormal after either 7 or 14 days in the low-glucose media (Figure 3), indicating that the acquired decrement in gap junctional communication could not be reversed within 2 weeks by simply reducing the glucose concentration in the culture medium.

Oxidative stress precedes impairment of gap junctional communication

Because diabetes is associated with oxidative stress (Brownlee, 2005), DCF fluorescence was assayed at intervals after exposure of astrocytes to the high-glucose medium to assess changes in the levels of ROS and RNS. Increased DCF fluorescence was detectable after 1 day of exposure to high glucose, with a progressive rise with time in culture (Figure 4). Elevated ROS/RNS production preceded impairment of gap junctional communication that became evident only after 3–5 days of exposure to very high glucose (compare Figures 2E, 2F and 4).

Focal oxidative stress

The high-glucose cultures had focal 'hot spots' of greater DCF fluorescence intensities (quantified by thresholding the highest 2% fluorescence values; see the Materials and methods section) that averaged approximately twice those of the overall mean intensities in the high-glucose cultures (thresholded at 30%) at all time points (Figure 4). The hot spots in the hyperglycaemic cultures also had quite large S.D. values. In contrast, hot spots in the control cultures grown in 5.5 mmol/l glucose had fluorescence intensities closer to the overall mean intensities (Figure 4).

Magnitude of oxidative stress is variable in culture batches

In a replicate experiment (results not shown) in which astrocytes were grown in high or low glucose for 1, 3, 7 or 14 days ($n=3$–5 coverslips per group with 9–11 regions of interest assayed per coverslip for a total of 44–70 regions per group) the cells were incubated for 30 min in 30 μmol/l DCF-DA, and at each time point, DCF fluorescence was statistically significantly higher in cells grown in 25 mmol/l glucose

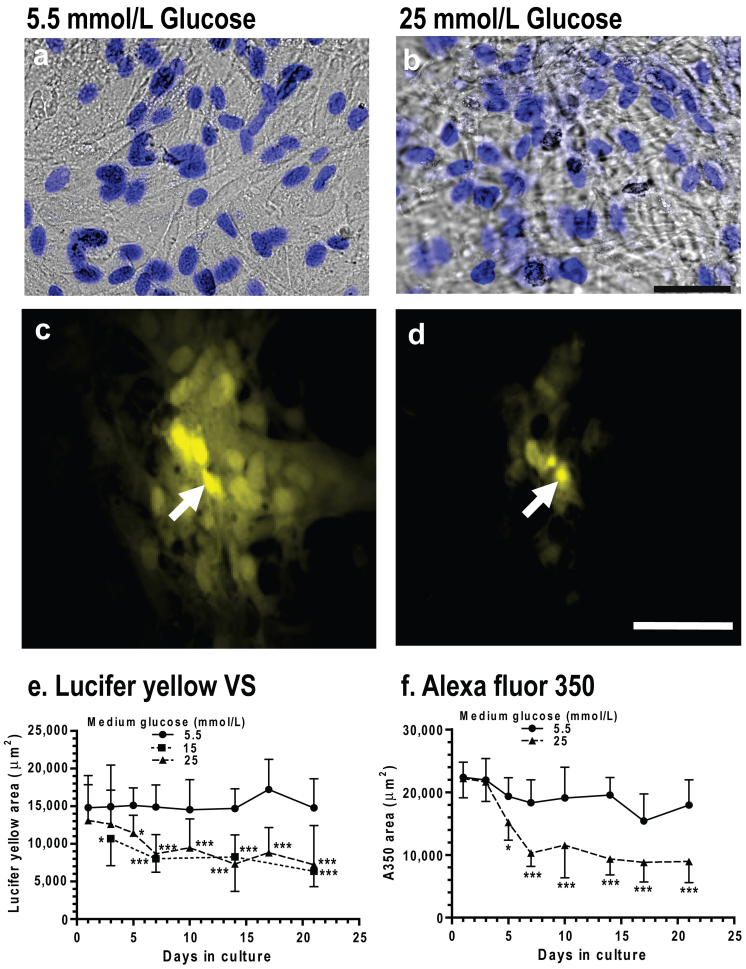

Figure 2 **Slow onset of dye transfer impairment in severely hyperglycaemic astrocytes**

Representative DIC images of astrocytes grown in 5.5 mmol/l (**A**) or 25 mmol/l (**B**) glucose for 14 days; images of nuclei that were stained with Hoechst dye are superimposed on the DIC images. Similar cell densities were found in the low-glucose (44 ± 8 cells per field) and high-glucose (42 ± 15 cells per field) cultures when the numbers of nuclei were counted on day 14 in images of different cultures in 15 random fields of view (i.e. 200 μm × 200 μm with a × 40 objective) per group. Dye-transfer was assayed by impaling a single astrocyte in different groups of cells with a micropipette, the dye was diffused into the cell for 2 min and the labelled area was measured (**C**–**F**). Representative images (**C**, **D**) illustrate diffusion of LYVS among astrocytes grown for 21 days in 5.5 mmol/l (**C**) or 25 mmol/l (**D**) glucose; arrows identify the impaled cell. The scale bars in (**B**) and (**D**) are 50 μm and also apply to images in (**A**) and (**C**). Dependence of Lucifer Yellow-labelled area on duration of growth at various glucose concentrations (**E**). The respective number of samples per group is as follows: 5.5 mmol/l glucose, $n=7$, 17, 6, 12, 16, 21, 10 and 21 at 1, 3, 5, 7, 10, 14, 17 and 21 days; 15 mmol/l glucose, $n=20$, 20, 20, 18 at 3, 7, 14 and 21 days; 25 mmol/l glucose, $n=8$, 18, 6, 14, 17, 21, 16, 23 at 1, 3, 5, 7, 10, 14, 17 and 21 days. Alexa Fluor® 350 (A350)-labelled area declines with time in high-glucose-containing medium (**F**). The respective number of samples per group at 1, 3, 5, 7, 10, 14, 17 and 21 days is as follows: 5.5 mmol/l glucose, $n=6$, 6, 7, 12, 18, 13, 12 and 11; 25 mmol/l glucose, $n=6$, 8, 6, 12, 19, 12, 10 and 12. Cells in each experimental group were derived from at least three independent cultures. Values are means and vertical bars represent 1 S.D.; bars that are smaller than the symbol are not visible. $^{*}P<0.05$, $^{**}P<0.01$, $^{***}P<0.001$, for the indicated comparisons using the unpaired, two-tailed *t* test for two groups, and ANOVA and Dunnett's test for multiple comparisons against the respective 5.5 mmol/l glucose group.

compared with those in 5.5 mmol/l glucose ($P<0.001$). However, the mean DCF fluorescence intensities in the high-glucose cultures were more similar to each other at each time point, differing somewhat from the data set in Figure 4. The high glucose/low glucose ratio of DCF values in the replicate cultures was 1.86, 2.84, 2.04 and 2.67 at 1, 3, 7 and 14 days for threshold at 30%, and 2.52, 4.02, 2.42, and 4.78 respectively for the 'hot spots' quantified by thresholding at 2%. Thus the high-glucose cultures have higher DCF fluorescence than those grown in low glucose, but replicate assays can differ in magnitude. For unidentified reasons, some astrocytes grown in high glucose exhibited low DCF fluorescence at 14 days, but they still had reduced trafficking of LYVS. Unfortunately, the oxidative stress and gap junctional transfer assays do not permit longitudinal studies on the same cells; the properties of the cells before the assay are unknown.

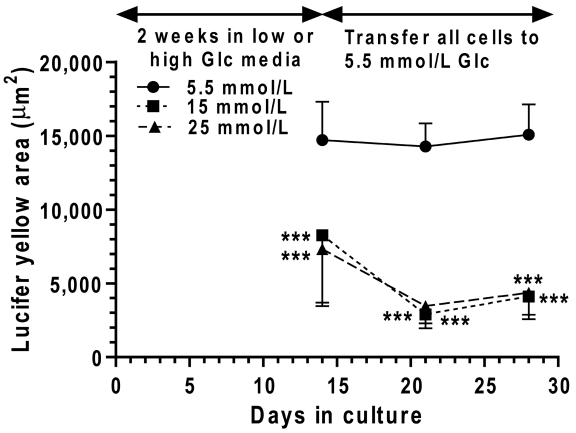

Figure 3 Glycaemic control does not reverse the deficit previously acquired during growth in hyperglycaemic conditions

Cultured astrocytes were grown in medium containing the indicated glucose concentrations for 14 days. Then the cells grown in 15 or 25 mmol/l glucose were also cultured in medium containing 5.5 mmol/l glucose, and all cultures continued for an additional 7 or 14 days. At the time intervals indicated, dye transfer was assayed by impaling a single astrocyte with a micropipette, dye was diffused into the cell for 2 min and labelled area was measured. The respective number of samples/group at 21 and 28 days is as follows: 5.5 mmol/l glucose, $n=20$ and 10; 15 mmol/l glucose, $n=10$ and 10; and 25 mmol/l glucose, $n=20$ and 10. Cells in each experimental group were derived from at least three independent cultures. Values are means and vertical bars represent 1 S.D.; when bars are not visible, they are smaller than the symbol. $^{*}P<0.05$, $^{**}P<0.01$, $^{***}P<0.001$, for the indicated comparisons using ANOVA and Dunnett's test for multiple comparisons against the respective 5.5 mmol/l glucose group.

Diabetic rat brain exhibits abnormal dye transfer and oxidative stress

The body weight of STZ-diabetic rats during the 13–20-week interval after onset of diabetes averaged 53 ± 2% ($n=4$) of age-matched, vehicle-injected controls ($n=4$), and at 20 weeks, the respective body weights were 268 ± 36 and 471 ± 19 g. At the time of assay for dye transfer and oxidative stress, the arterial plasma glucose level in diabetic rats was elevated 4.1-fold compared with controls (33.1 ± 5.2 and 8.0 ± 0.9 mmol/l respectively; $P<0.001$), whereas arterial plasma lactate content was unchanged (2.2 ± 0.7 and 2.2 ± 0.4 mmol/l respectively). To verify that brain glucose levels were also elevated in our STZ rats, the glucose concentration was assayed in ethanol extracts of cerebral cortex dissected from funnel-frozen brains of two STZ rats, using previously described methods (Dienel et al., 2007). The brain glucose concentrations were 8.2 and 6.8 μmol/g, indicating that both plasma and brain glucose levels in the STZ rats used in the present study were within the range of the mean literature values tabulated in Table 1.

Dye transfer among gap junction coupled astrocytes was assayed by dye diffusion into single astrocytes in slices of the inferior colliculus from age-matched, vehicle-treated control and STZ-diabetic rats. Both Lucifer Yellow and 6-NBDG had greater dye labelling in slices from control rats (Figures 5A and 5C) compared with those from STZ-treated rats (Figures 5B and 5D). The number of LYVS-labelled cells was

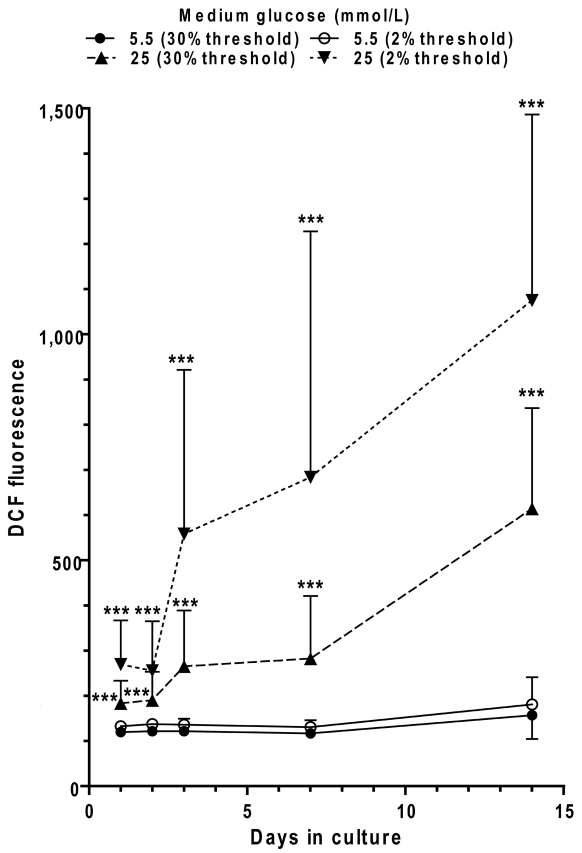

Figure 4 Oxidative stress is detectable after 1 day of severe hyperglycaemia and remains elevated

Cultured astrocytes were grown in media containing 5.5 or 25 mmol/l glucose for 14 days. ROS/RNS production was assayed by DCF fluorescence (30 min incubation in 10 μmol/l DCFDA) and quantified using MetaVue software, with thresholding to include either the highest 2% or 30% fluorescence intensities; thresholding at 30% excluded the background and thresholding at 2% quantified the small 'hot spots' that are readily visible in the images. The values thresholded at 2% and 30% were similar for cells grown in 5.5 mmol/l glucose; comparisons between the cells grown in 5.5 or 25 mmol/l glucose were made for each respective threshold value. Endogenous fluorescence in the absence of DCF was 114 ± 3 (30% threshold) and 123 ± 5 (2% threshold) for cells grown in 5.5 mmol/l glucose for 3 or 7 days, and slightly lower values were obtained for cells grown in 25 mmol/l glucose (results not shown). These control values for endogenous fluorescence were not subtracted from those in which DCF was added to assay NOS/ROS production, indicating that generation of DCF fluorescence by reactive species in low-glucose media is very low. The respective number of samples per group at 1, 2, 3, 7 and 14 days is as follows: 5.5 mmol/l glucose, $n=30$, 29, 30, 30 and 45; 25 mmol/l glucose, $n=20$, 17, 29, 15 and 35. Each sample represents analyses of images (200μm $\times$ 200 μm) of astrocytes grown on coverslips; results are from up to ten images per coverslip and three to five coverslips per group. Cells in each experimental group were derived from at least three independent cultures. Values are means and vertical bars represent 1 S.D.; when bars are not visible, they are smaller than the symbol. $^{***}P<0.001$, for the indicated comparisons using the unpaired, two-tailed t test against the respective 5.5 mmol/l glucose group.

7.7-fold higher in slices from control compared with diabetic rats (Figure 6A), whereas the area labelled by the fluorescent glucose analogue, 6-NBDG (342 Da), was 2.2-fold greater in control compared with diabetic rat slices (Figure 6B). DCF fluorescence in diabetic brain slices was 3.2 times that in controls (Figure 6C). Thus gap junctional communication was

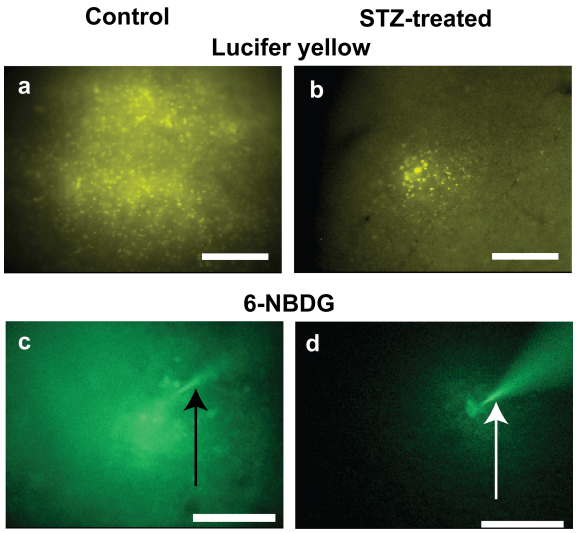

Figure 5 Reduced dye transfer among astrocytes in brain slices from STZ-diabetic rats compared with controls

Gap junctional communication was assayed in slices of inferior colliculus from age-matched, vehicle-injected controls (**A**, **C**) and STZ-diabetic rats at 20–24 weeks after the onset of diabetes (**B**, **D**). A single astrocyte was impaled with a micropipette containing either Lucifer Yellow (**A**, **B**) or 6-NBDG (**C**, **D**), and the dye was diffused into the cell for 5 min. The Lucifer Yellow was a mixture of LYVS (4 g/100 ml)+LYCH (4 g/100 ml). 6-NBDG (5 mmol/l) is a non-metabolizable fluorescent analogue of glucose. The scale bars in (**A**, **B**) are 200 μm (imaged with a ×10 objective), and those in (**C**, **D**) are 40 μm (imaged with a ×40 objective). Arrows in (**C**, **D**) indicate the NBDG-containing micropipette.

reduced and oxidative stress was increased in slices of the inferior colliculus from diabetic rats at 20–24 weeks after STZ treatment, as observed in cultured astrocytes that were exposed to much higher glucose levels for short time intervals (compare with Figures 2 and 4).

Pharmacological treatment can induce, prevent or restore changes in gap junctional permeability

ER stress is associated with obesity, insulin resistance and Type 2 diabetes, and treatment with chemical chaperones that reduce ER stress normalizes many pathophysiological consequences of Type 2 diabetes (Özcan et al., 2004, 2006). A toxin that induces ER stress, ROS/NOS blockers that can reduce oxidative stress (Cruthirds et al., 2005) and chemical chaperones known to facilitate protein folding (Welch and Brown, 1996; Özcan et al., 2006) were, therefore, tested for their ability to cause, prevent or restore deficits in gap junctional communication.

ER stress impairs gap junctional communication

Tunicamycin is an inhibitor of *N*-acetylglucosamine transferases known to cause ER stress by blocking the formation of *N*-glycosidic protein–carbohydrate linkages and preventing the glycosylation of newly synthesized proteins in the ER. Astrocytes were grown for 2 weeks in low glucose and then treated with

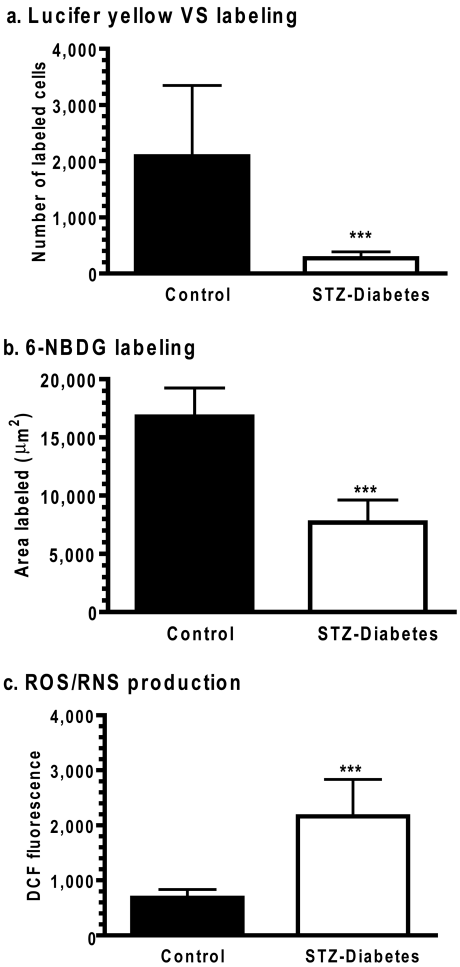

Figure 6 Gap junctional communication and oxidative stress in brain slices from control and STZ-diabetic rats

Dye transfer was assayed in slices of inferior colliculus from adult male rats at 20–24 weeks after the onset of STZ-induced diabetes and in age-matched, vehicle-injected controls by impaling a single astrocyte with a tracer-containing micropipette and diffusing the tracer for 5 min (for more details, see the legend to Figure 5). (**A**) Cells labelled with LYVS+LYCH (n=19, with 1 injection into each of 19 brain slices derived from 4 control rats and 19 slices from four diabetic rats). (**B**) Area labelled with 6-NBDG (n=20 injections into ten slices from five control rats and 16 injections into eight slices from four diabetic rats). Note that the NBDG-labelled areas were measured in slices while viewing with a ×40 objective because the area labelled in the STZ-rat slices was difficult to determine with a ×10 objective; the NBDG-labelled area in the control rats was, therefore, probably underestimated (see Figure 5) and the difference between control and diabetic rats is likely to be greater than shown in (**B**). (**C**) Formation of ROS/RNS species in slices of inferior colliculus from control (n=10) and STZ-diabetic (n=8) rats was assayed as carboxy-DCF fluorescence. ***P<0.001, unpaired, two-tailed t tests.

tunicamycin for 16 h and dye transfer was assayed. The dye-labelled area was reduced by tunicamycin to the low level observed in vehicle-treated cells that were grown in high glucose for 2 weeks (Figure 7A), i.e. the Lucifer Yellow-labelled area was approx. 4000 μm^2 under both these conditions. For comparison with these values, astrocytes grown in low glucose for up to 3 weeks had a Lucifer Yellow-labelled area of approx. 15 000 μm^2 (Figures 2 and 3) and the 2–3 week values for low-glucose cultures from Figures 2 and 3 are included in

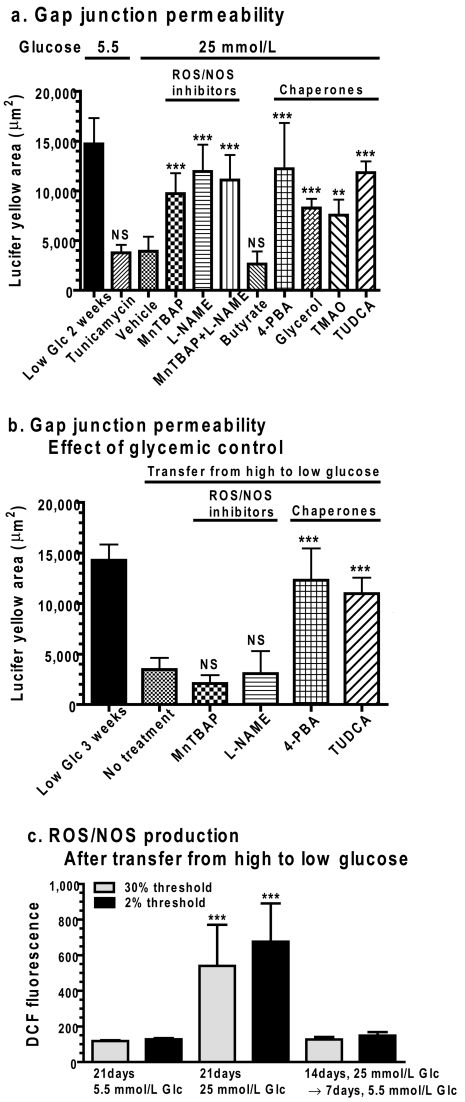

Figure 7 Influence of ROS/NOS inhibitors and chemical chaperones on dye transfer and DCF fluorescence

(**A**) Dye transfer after diffusion into a single cell for 2 min was assayed in astrocytes grown in high glucose for 14 days in the presence of various compounds that were added to the culture medium at the onset of culture in high glucose or (**B**) after 2 weeks growth in high glucose, followed by culture for 1 week in low-glucose medium that contained inhibitors or chaperones. For reference, the dye-labelled area obtained in low-glucose cultures grown for 2 weeks (results from Figure 2E) are included in (**A**), and that from low-glucose cultures at 3 weeks (results from Figure 3) are included in (**B**). However, statistical comparisons did not include these data to avoid additional multiple comparisons against the same data sets in other Figures. (**C**) DCF fluorescence was assayed in astrocytes after 3 weeks growth in low or high glucose (Glc) or 2 weeks in only high-glucose media followed by 1 week in low glucose. DCF fluorescence was thresholded at 30% or 2% of fluorescence intensity as described in the caption of Figure 4 to quantify the overall response and 'hot spots' respectively. Values are means and vertical bars represent 1 S.D. Statistical comparisons, denoted as NS, not significant; $^{*}P<0.05$; $^{**}P<0.01$; $^{***}P<0.001$, were as follows. In (**A**), multiple comparisons were made with ANOVA and Dunnett's test against the vehicle-treated 25 mmol/l glucose culture [$n=25$, 13, 24, 22, 5, 15, 25, 12, 8 and 5 for the vehicle (0.1 mol/l PBS), MnTBAP (50 μmol/l), L-NAME (1 mmol/l), MnTBAP (50 μmol/l)+L-NAME (1 mmol/l), tunicamycin (100 ng/ml for 16 h), butyrate (1 mmol/l), 4-PBA (1 mmol/l), glycerol (25 mmol/l), TMAO (100 mmol/l) and TUDCA (25 mmol/l) groups respectively]. In (**B**), comparisons were made against the no-treatment group that was transferred from high to low glucose ($n=20$, 10, 10, 12 and 8 for the no treatment, MnTBAP, L-NAME, 4-PBA and TUDCA groups respectively). In (**C**), comparisons were against the 5.5 mmol/l glucose group ($n=30$ for 21 day/5.5 mmol/l; $n=20$ for 21 day/25 mmol/l; $n=30$ for 14 day/25 mmol/l followed by 7 day/5.5 mmol/l).

Figures 7(A) and 7(B) as reference values. However, to avoid additional multiple statistical comparisons against the same data sets, comparisons in Figures 7(A) and 7(B) were made against the vehicle-treated control grown in high glucose or the no treatment group in the high-to-low glucose transfer assay.

ROS/RNS inhibitors and chemical chaperones are protective in the presence of high glucose

Continuous 2-week treatment of cultured astrocytes grown in high glucose with MnTBAP, a superoxide dismutase mimetic, or with L-NAME, an inhibitor of NOS (alone or in combination) prevented the high-glucose-induced decrement in dye transfer (Figure 7A). Similarly, four chemically different chaperone molecules (4-PBA, glycerol, TMAO and TUDCA) also protected against dye transfer impairment, whereas butyrate, a control for 4-PBA, did not (Figure 7A).

Chaperones, not ROS/RNS inhibitors, restore the acquired deficit

Astrocytes were grown for 2 weeks in high glucose and then transferred to the low-glucose medium containing vehicle or other compounds for 7 days. The dye-labelled area in vehicle-treated astrocytes remained at the low level (Figure 7B) obtained for astrocytes previously grown in high glucose (compare with Figure 3). Inclusion of MnTBAP or L-NAME in the low-glucose medium did not restore gap junctional trafficking (i.e. the dye-labelled area remained low), whereas inclusion of two chaperones, 4-PBA and TUDCA, did improve dye transfer and increased the labelled area (Figure 7B).

Oxidative stress is eliminated by transfer to low glucose

DCF fluorescence was elevated in cells grown in high glucose for 3 weeks compared with those grown in low glucose. However, when astrocytes were grown in high glucose for 2 weeks and then transferred to low glucose for an additional week, the level of oxidative stress fell to that of cells continuously grown in low glucose for 3 weeks (Figure 7C). Thus the decrement in gap junctional communication caused by prior exposure to high glucose persists (Figure 7B, no treatment group), even though oxidative stress is eliminated (Figure 7C) by reducing the glucose level in the culture medium.

Effect of gap junction permeability modulators on oxidative stress

The ROS/RNS blockers would be expected to improve gap junctional communication by reducing or preventing the rise

in DCF fluorescence in cells grown in high glucose, whereas the chaperone molecules would not be expected to alter glucose-induced oxidative stress. To test these predictions, DCF fluorescence was assayed in two independent experiments using different batches of astrocytes that were grown for 2 weeks in 25 mmol/l glucose in the continuous presence of each of the test compounds shown in Figure 7(A) (n=30–40 samples per group per experiment). Unfortunately, the results in the replicate assays were variable (results not shown), and further work is required to identify factors that influence the response of DCF fluorescence intensity to these drug treatments.

Summary of results of pharmacological studies

Both prolonged exposure to high glucose and short-term tunicamycin treatment impair astrocytic gap junctional communication. In high-glucose cultures, oxidative stress is detectable on day 1 (Figure 4), whereas the fall in dye transfer becomes manifest at approx. 3–5 days (Figures 2E and 2F). Transfer of cells from high- to low-glucose medium was sufficient to reduce DCF fluorescence to control levels (Figure 7C), but not restore dye transfer to normal within 2 weeks (Figure 3). ROS/RNS inhibitors could prevent this deficit if included in the medium at the onset of exposure to high glucose (Figure 7A), but could not improve the acquired deficit that persisted in the low-glucose medium (Figure 7B). Chaperone treatment could, however, restore the gap junctional deficit in the presence of high glucose (Figure 7A), as well as in the presence (Figure 7A) or absence (Figures 7B and 7C) of elevated DCF fluorescence. Thus prolonged antecedent oxidative stress is linked to reduced gap junctional trafficking, but reducing ROS/RNS levels after the onset of the deficit did not restore dye transfer (Figure 3). In sharp contrast, the persistent change in Cx function acquired by growth in high glucose was ameliorated by four different chaperone molecules that can improve protein folding

Immunoreactive Cx protein

All astrocytes exhibited immunostaining for Cx43, Cx30 and Cx26, with the most intense immunoreactivity mainly in intracellular material, as illustrated for astrocytes grown for 2 weeks in 5.5 mmol/l glucose (Figure 8, left column). Intracellular immunostained Cx protein can include ER, Golgi apparatus and cytoplasmic vesicles (Wolff et al., 1998 and references cited therein), and punctate, vesicle-like intracellular staining in astrocytes is evident in other studies (e.g. Ye et al., 2003). The area of the immunoreactive punctate structures in astrocytes grown in high glucose was reduced to approx. 50% and 25% of that in the low-glucose cultures respectively for Cx43 and Cx30, whereas that for Cx26 was unaffected (Figure 8, right column). Thus the morphological appearance of immunoreactive Cx protein is selectively influenced by medium glucose concentration, perhaps reflecting changes in trafficking or turnover of these proteins.

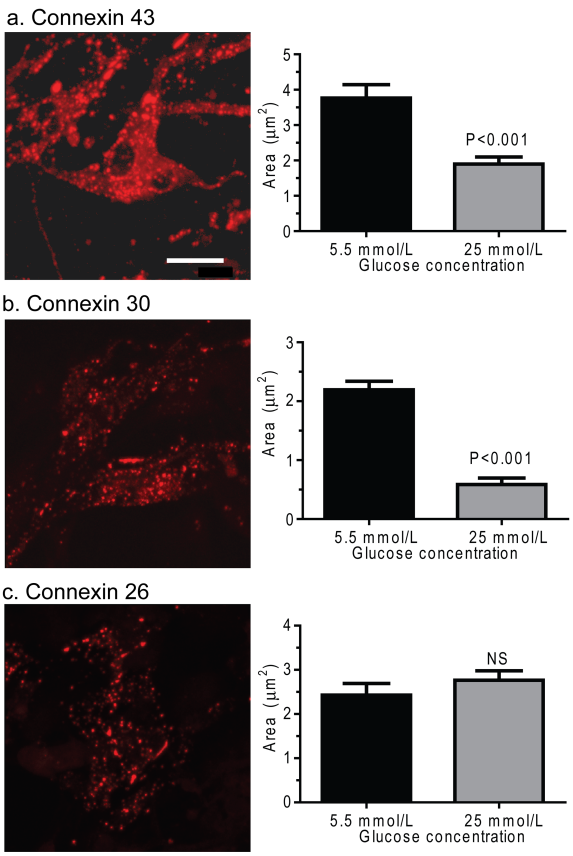

Figure 8 Effect of hyperglycaemia on staining of immunoreactive Cx proteins in cultured astrocytes

Composite z-stacks of confocal images (left column) of immunostained astrocytes showed a low-intensity background and prominent staining of punctate or vesicular immunoreactive material that appeared to be mainly intracellular. This morphological appearance of immunostaining was evident for Cx43 (**A**), Cx30 (**B**) and Cx26 (**C**) protein in astrocytes grown on coverslips for 14 days in a medium containing 5.5 mmol/l glucose; the scale bar is 12.5 μm and applies to all panels. Areas of these immunostained punctate/vesicular objects (right columns) are means (vertical bars represent 1 S.D.) from the following numbers of objects per group: Cx43, 5.5 mmol/l: n=752 objects in cells on five coverslips; 25 mmol/l: n=884 objects in cells on five coverslips; Cx30, 5.5 mmol/l: n=1099 objects, five coverslips; 25 mmol/l: n=1177 objects, five coverslips; Cx26, 5.5 mmol/l: n=514 objects, four coverslips; and 25 mmol/l: n=974 objects, five coverslips.

DISCUSSION

Prolonged hyperglycaemia interferes with astrocytic gap junctional communication

The two major findings of the present study are that chronic hyperglycaemia and STZ-induced diabetes markedly reduce gap junctional dye transfer among astrocytes and that the impairment of gap junctional communication can be prevented and rescued by pharmacological treatment with compounds that reduce oxidative stress or improve protein folding. Impaired transcellular communication had a slow onset and, once established, it was poorly reversible by

subsequent glycaemic control. This deficit was detectable with three tracers of different sizes and charges (Lucifer Yellow, Alexa Fluor® 350 and 6-NBDG, a non-metabolizable glucose analogue), and the scrape-loading assays indicate that it did not arise from differential dye release by hyperglycaemic cells via pannexin pores or Cx hemichannels (Figures 1–3). Because increased DCF fluorescence preceded the onset of the decline in gap junctional permeability by 3–5 days and ROS/RNS blockers could prevent but not rescue the decrement (Figures 4 and 7), damage arising from oxidative stress may be a causative factor. Acute tunicamycin treatment generates abnormal newly synthesized proteins, causes ER stress and impairs dye transfer within 16 h without hyperglycaemia and oxidative stress. However, results of our ongoing studies indicate that expression of selected markers for ER stress is delayed compared with onset of reduced gap junctional communication in hyperglycaemic cultured astrocytes, suggesting that gap junctional impairment may be an early, relatively selective event in the pathophysiology of diabetes.

High glucose is sufficient to impair gap junctional communication

The effects of chronic hyperglycaemia and complications of diabetes are very complex, and relationships among pathophysiology, threshold glucose level and cumulative exposure to elevated glucose concentrations are very difficult to define. However, tissue culture experiments demonstrate that severe, chronic hyperglycaemia itself is sufficient to disrupt gap junctional communication in astrocytes in the absence of endocrine dysfunction and multiorgan interactions. Both of our experimental model systems, cultured astrocytes and STZ-rats, have high glucose concentration as a variable, but they differ with respect to maximal glucose level, cumulative exposure and effects of interactions among brain cell types and among body organs. Cumulative exposure can be expressed as the product of glucose concentration multiplied by time, or the area under a plot of concentration as a function of time. Different pathophysiological processes can be expected to take place at various threshold levels of glucose concentration. For example, glucose flux into the sorbitol pathway will progressively increase as glucose concentration rises above normal due to the high K_m of aldose reductase for glucose (~25 mM). The threshold concentrations and cumulative exposure required to cause various effects of elevated glucose (e.g. non-enzymatic glycation reactions, oxidative stress and disruption of signalling pathways) are unknown, but these effects could be expected to increase with glucose level and duration of exposure (Mîinea et al., 2002). Brain glucose levels are lower than in peripheral tissues owing to the restrictive transport properties of the blood–brain barrier (Table 1), but diabetic patients live with the disease for decades, facilitating cumulative CNS (central nervous system) effects of chronic hyperglycaemia.

Growth of cultured cells under severely hyperglycaemic conditions is a pathophysiological condition relevant to diabetes. Commercially available tissue culture media can contain glucose concentrations ranging from 0 to 25 mmol/l and, for example, DMEM is formulated with 0, 5.56 or 25 mmol/l glucose, Ham's nutrient mixtures can have 7, 10 or 17.5 mmol/l glucose and Neurobasal™ medium (Brewer et al., 1993) contains 25 mmol/l glucose. Even a 'low-glucose' medium, 5–6 mmol/l glucose, is approximately twice the normal rat brain glucose concentration (i.e. approx. 2–3 μmol/g) and is equivalent to severe diabetes in rat brain (Table 1). Growth of astrocytes in 22 mmol/l glucose reduces both glucose and lactate oxidation by approx. 50% compared with cells grown in 2 mmol/l glucose (Abe et al., 2006), and would be expected to predispose astrocytes grown in high glucose to increased glycolytic metabolism and greater lactate release. In cultured neurons, the lactate dehydrogenase isoenzyme pattern was not altered by medium glucose level (5.5, 13.4 or 26.8 mmol/l; O'Brien et al., 2007), but Kleman et al. (2008) emphasize the negative effects of high glucose levels on the viability of cultured neurons and neuronal responsiveness to the AMPK (AMP-activated protein kinase) energy signalling system. High glucose may or may not influence experimental outcome, but diabetic complications are, nevertheless, a concern for astrocytes and neurons grown in high glucose, and it is important to re-evaluate the results of such studies (e.g. 20 mmol/l glucose: Ye et al., 2001, 2003, 2009; McCoy and Sontheimer, 2010; 25 mmol/l glucose: Sorg and Magistretti, 1991; Yu et al., 1993; Takahashi et al., 1995; Itoh et al., 2003; Pellerin and Magistretti, 2005, 1994; Chenal and Pellerin, 2007; and 50 mmol/l glucose: Bliss et al., 2004). Also, Methods sections in published studies sometimes only identify the 'generic' culture medium (e.g. DMEM) without stating the glucose level or other key constituents; ideally, the catalogue number of the medium should be reported so its formulation is available. The use of normal brain tissue glucose levels for growth of cultured cells with twice-weekly feeding schedules may also have nutritional complexities. For example, our unpublished data (K.K. Ball, N.F. Cruz and G.A. Dienel) indicate that astrocytes grown in 5.5 mmol/l glucose consume most of the glucose within approx. 12–18 h, with release of lactate to the medium; this lactate can be subsequently consumed as an oxidative substrate, along with glutamine and other substrates in the medium. Daily replenishment of glucose and other nutrients and removal of lactate and other compounds released to the culture medium may be necessary to control levels of extracellular metabolites, but total medium replacement could also negatively affect the cells due to various 'stresses' associated with removal from the incubator and medium change, e.g. shear stress to the surface of the cells, transient loss of CO_2 and buffering capacity, and transient hypoxia and hypothermia.

Abnormal proteins and therapeutic potential

Covalent protein modification can arise from various causes known to occur in diabetes, e.g. non-enzymatic glycation

reactions and formation of advanced glycation end-products, protein carbonylation reactions, and altered regulation of gene expression and signalling pathways causing abnormal phosphorylation or nitrosylation states (Bonnefont-Rousselot, 2002; Brownlee, 2005). The ability of four different chaperone molecules that can facilitate protein folding in other experimental systems to (i) prevent the decline in dye transfer even in the presence of high glucose levels and oxidative stress and (ii) rescue an established deficit (Figure 7) suggests that changes to Cx proteins secondary to oxidative stress may cause abnormal protein structure, folding, protein–protein interactions or protein trafficking that may be reflected by the morphological changes in intracellular non-junctional immunoreactive Cx 43 and 30 protein (Figure 8). Further work is required to evaluate the contributions of these possibilities to altered non-junctional immunoreactive material in diabetic astrocytes. Poor reversibility of gap junctional communication after reversion to low-glucose culture media (Figures 3 and 7B) underscores the importance of continuous, strict glycaemic control in diabetic patients. The effectiveness of treatment with chaperones (Figure 7) that are already approved for human use (e.g. 4-phenylbutyrate and TUDCA; Özcan et al., 2006) opens a therapeutic avenue to improve gap junctional intercellular trafficking that is effective in the presence of high glucose levels, oxidative stress and metabolic disturbances.

Involvement of different Cxs in many cell types during experimental diabetes

Dysfunction of any or all the three astrocytic Cxs (Cx43, Cx30 and Cx26), as well as Cx-associated proteins, may contribute to the functional deficit of gap junctional trafficking of small molecules during experimental diabetes and would be anticipated to affect transcellular communication via channels that comprise these Cxs in all body tissues, not just brain. Because Cx30 channels are not permeable to LYCH (Manthey et al., 2001), the abnormal transfer of Lucifer Yellow may involve Cx43 and Cx26 channels that are permeant to this dye (Elfgang et al., 1995). Cx43 may be a major 'target' of diabetes in astrocytes, as well in other organs, as suggested by previous studies in other cell types.

Gap junctional communication in a number of cell types is inhibited by growth in high-glucose media ranging from 14 to 30 mmol/l for different intervals (1–9 days) compared with cells grown in 5–5.5 mmol/l glucose, and decrements have been documented in endothelial cells in the aorta (Inoguchi et al., 1995, 2001), in the retina (Fernandes et al., 2004) and in epididymal fat pads (Sato et al., 2002; Li and Roy, 2009), in smooth muscle cells in aorta (Kuroki et al., 1998; Inoguchi et al., 2001), in pigment epithelial cells in retina (Stalmans and Himpens, 1997; Malfait et al., 2001), and in pericytes in retina (Li et al., 2003). These studies have linked dye transfer deficits to altered PKC (protein kinase C) signalling, increased phosphorylation of Cx43, reduced Cx43 mRNA and protein levels, low Cx43 plaque counts, and increased proteosome-mediated degradation of Cx43. Consistent with the above findings are reports that propagation of calcium waves is inhibited in hyperglycaemic and PKC-activated retinal pigment epithelial cells (Stalmans and Himpens, 1997), as well as in PKC-activated astrocytes (Enkvist and McCarthy, 1992). In STZ-diabetic rats, dye transfer is reduced in acutely isolated pericytes in retinal microvessels after 5–18 days of diabetes (Oku et al., 2001). Also, the increased duration of QRS waves in electrocardiograms from STZ-diabetic rats is associated with increased phosphorylation of Cx43 that is linked to activation of PKC, with either unchanged or reduced Cx43 protein levels (Inoguchi et al., 2001; Lin et al., 2006, 2008; Howarth et al., 2008). However, in coronary endothelial cells isolated from STZ-diabetic mice, Cx40 is a critical element in loss of gap junction intercellular communication; its levels are reduced, along with those of Cx37, but not Cx43, and high glucose impairs capillary network formation *in vitro* (Makino et al., 2008). Together, the above findings indicate that gap junctional communication is abnormal in many organ systems exposed to prolonged hyperglycaemia and experimental diabetes, with tissue- and organ-specific effects. The brain is generally considered to be affected by diabetes to a lesser extent than peripheral organs, but gap junctional trafficking among astrocytes, retinal cells and endothelial cells is markedly reduced.

Roles of gap junctions in pathophysiology of diabetes and Alzheimer's disease

Gap junction-coupled astrocytes are involved in integration of neurotransmission, energetics and blood flow at a local level, and impaired syncytial communication by means of cytoplasmic signalling, redox and energy-related molecules can contribute to brain dysfunction. For example, lack of Ins(1,4,5)P_3 signalling arising from mutations in Cx26 in non-neuronal support cells in the cochlea is sufficient to cause deafness (Beltramello et al., 2005), indicating that a sensory loss associated with neurons can arise from dysfunction of other cell types whose roles are required for processing of sensory information. Gap junctions have important roles in regulation of vascular function (Figueroa and Duling, 2009), and the brain's vasculature is surrounded by astrocytic endfeet that are extensively coupled with each other by gap junctions that facilitate long-distance dye transfer along the vasculature when dye is diffused into a single astrocyte (Ball et al., 2007). Thus it is likely that signals among cells within the 'neurovascular unit' that comprises neurons, astrocytes and endothelial cells would be disrupted by impairment of gap junctional communication between astrocytic processes and their endfeet. As discussed above, hyperglycaemia induces abnormalities in Cx proteins and signalling in astrocytes, endothelial cells in different tissues, vascular smooth muscle cells, and retinal pericytes. Microvascular pathology is common to diabetes and Alzheimer's disease (Luchsinger and Gustafson,

2009; Sonnen et al., 2009), STZ-diabetic rats exhibit increased levels of amyloid β-peptide and phosphorylated tau protein (Li et al., 2007), hyperglycaemia exacerbates pathophysiological changes and cognitive decline in pre-symptomatic Alzheimer's mice (Burdo et al., 2009), and aged Alzheimer model mice have altered astrocytic networks (Peters et al., 2009). Taken together, these findings suggest that impairment of astrocytic gap junctional trafficking may contribute to the pathology of the microvasculature in brain and, ultimately, to sensory and cognitive decline in diabetes and Alzheimer's disease. In addition, involvement of abnormalities in gap junctional communication in vascular endothelial and smooth muscle cells and cardiac cells may underlie or contribute to complications of diabetes in the cardiovascular system and other organs.

FUNDING

This work was supported by NIH (National Institutes of Health) [grant numbers NS36728, NS47546 and DK081936]; Alzheimer Foundation [IIRG-06-26022]; and the University of Arkansas for Medical Sciences Department of Physiology and Biophysics, Graduate School, and Research Council. The content of the present work is solely the responsibility of the authors and does not necessarily represent the official views of the National Institute of Neurological Disorders and Stroke, the National Institute of Diabetes and Digestive and Kidney Diseases, or the NIH.

REFERENCES

Abe T, Takahashi S, Suzuki N (2006) Oxidative metabolism in cultured rat astroglia: effects of reducing the glucose concentration in the culture medium and of D-aspartate or potassium stimulation. J Cereb Blood Flow Metab 26:153–160.

Allen KV, Frier BM, Strachan MW (2004) The relationship between type 2 diabetes and cognitive dysfunction: longitudinal studies and their methodological limitations. Eur J Pharmacol 490:169–175.

Ball KK, Gandhi GK, Thrash J, Cruz NF, Dienel GA (2007) Astrocytic connexin distributions and rapid, extensive dye transfer via gap junctions in the inferior colliculus: implications for [^{14}C]glucose metabolite trafficking. J Neurosci Res 85:3267–3283.

Beltramello M, Piazza V, Bukauskas FF, Pozzan T, Mammano F (2005) Impaired permeability to Ins(1,4,5)P_3 in a mutant connexin underlies recessive hereditary deafness. Nat Cell Biol 7:63–69.

Biessels GJ, Gispen WH (2005) The impact of diabetes on cognition: what can be learned from rodent models? Neurobiol Aging 26 (Suppl. 1):36–41.

Biessels GJ, Kamal A, Urban IJ, Spruijt BM, Erkelens DW, Gispen WH (1998) Water maze learning and hippocampal synaptic plasticity in streptozotocin-diabetic rats: effects of insulin treatment. Brain Res 800:125–135.

Biessels GJ, Cristino NA, Rutten GJ, Hamers FP, Erkelens DW, Gispen WH (1999) Neurophysiological changes in the central and peripheral nervous system of streptozotocin-diabetic rats. Course of development and effects of insulin treatment. Brain 122:757–768.

Biessels GJ, ter Laak MP, Kamal A, Gispen WH (2005) Effects of the Ca^{2+} antagonist nimodipine on functional deficits in the peripheral and central nervous system of streptozotocin-diabetic rats. Brain Res 1035:86–93.

Blackshear PJ, Alberti KG (1974) Experimental diabetic ketoacidosis. Sequential changes of metabolic intermediates in blood, liver, cerebrospinal fluid and brain after acute insulin deprivation in the streptozotocin-diabetic rat. Biochem J 138:107–117.

Bliss TM, Ip M, Cheng E, Minami M, Pellerin L, Magistretti P, Sapolsky RM (2004) Dual-gene, dual-cell type therapy against an excitotoxic insult by bolstering neuroenergetics. J Neurosci 24:6202–6208.

Bonnefont-Rousselot D (2002) Glucose and reactive oxygen species. Curr Opin Clin Nutr Metab Care 5:561–568.

Brands AM, Biessels GJ, Kappelle LJ, de Haan EH, de Valk HW, Algra A, Kessels RP (2007) Utrecht Diabetic Encephalopathy Study Group. Cognitive functioning and brain MRI in patients with type 1 and type 2 diabetes mellitus: a comparative study. Dement Geriatr Cogn Disord 23:343. 9743771330–350.9743771330

Brewer GJ, Torricelli JR, Evege EK, Price PJ (1993) Optimized survival of hippocampal neurons in B27-supplemented Neurobasal, a new serum-free medium combination. J Neurosci Res 35:567–576.

Brown CR, Hong-Brown LQ, Biwersi J, Verkman AS, Welch WJ (1996) Chemical chaperones correct the mutant phenotype of the delta F508 cystic fibrosis transmembrane conductance regulator protein. Cell Stress Chaperones 1:117–125.

Brownlee M (2005) The pathobiology of diabetic complications: a unifying mechanism. Diabetes 54:1615–1625.

Buller N, Laurian N, Shvili I, Laurian L (1986) Delayed brainstem auditory evoked responses in experimental diabetes mellitus. J Laryngol Otol 100:883–891.

Buller N, Shvili Y, Laurian N, Laurian L, Zohar Y (1988) Delayed brainstem auditory evoked responses in diabetic patients. J Laryngol Otol 102:857–860.

Burdo JR, Chen Q, Calcutt NA, Schubert D (2009) The pathological interaction between diabetes and presymptomatic Alzheimer's disease. Neurobiol Aging 30:1910–1917.

Chenal J, Pellerin L (2007) Noradrenaline enhances the expression of the neuronal monocarboxylate transporter MCT2 by translational activation via stimulation of PI3K/Akt and the mTOR/S6K pathway. J Neurochem 102:389–397.

Cruthirds DL, Saba H, MacMillan-Crow LA (2005) Overexpression of manganese superoxide dismutase protects against ATP depletion-mediated cell death of proximal tubule cells. Arch Biochem Biophys 437:96–105.

DCCT/EDIC – Diabetes Control and Complications Trial/Epidemiology of Diabetes Interventions and Complications Study Research Group, Jacobson AM, Musen G, Ryan CM, Silvers N, Cleary P, Waberski B, Burwood A, Weinger K, Bayless M, Dahms W, Harth J (2007) Long-term effect of diabetes and its treatment on cognitive function. N Engl J Med 356:1842–1852.

Díaz de León-Morales LV, Jáuregui-Renaud K, Garay-Sevilla ME, Hernández-Prado J, Malacara-Hernández JM (2005) Auditory impairment in patients with type 2 diabetes mellitus. Arch Med Res 36:507–510.

Dienel GA, Cruz NF, Mori K, Holden JE, Sokoloff L (1991) Direct measurement of the lambda of the lumped constant of the deoxyglucose method in rat brain: determination of lambda and lumped constant from tissue glucose concentration or equilibrium brain/plasma distribution ratio for methylglucose. J Cereb Blood Flow Metab 11:25–34.

Dienel GA, Cruz NF, Adachi K, Sokoloff L, Holden JE (1997) Determination of local brain glucose level with [^{14}C]methylglucose: effects of glucose supply and demand. Am J Physiol 273:E839–E849.

Dienel GA, Ball KK, Cruz NF (2007) A glycogen phosphorylase inhibitor selectively enhances local rates of glucose utilization in brain during sensory stimulation of conscious rats: implications for glycogen turnover. J Neurochem 102:466–478.

Di Mario U, Morano S, Valle E, Pozzessere G (1995) Electrophysiological alterations of the central nervous system in diabetes mellitus. Diabetes Metab Rev 11:259–277.

Dodt HU, Zieglgänsberger W (1990) Visualizing unstained neurons in living brain slices by infrared DIC-videomicroscopy. Brain Res 537:333–336.

Elfgang C, Eckert R, Lichtenberg-Fraté H, Butterweck A, Traub O, Klein RA, Hülser DF, Willecke K (1995) Specific permeability and selective formation of gap junction channels in connexin-transfected HeLa cells. J Cell Biol 129:805–817.

el-Fouly MH, Trosko JE, Chang CC (1987) Scrape-loading and dye transfer: a rapid and simple technique to study gap junctional intercellular communication. Exp Cell Res 168:422–430.

Enkvist MO, McCarthy KD (1992) Activation of protein kinase C blocks astroglial gap junction communication and inhibits the spread of calcium waves. J Neurochem 59:519–526.

Fernandes R, Girão H, Pereira P (2004) High glucose down-regulates intercellular communication in retinal endothelial cells by enhancing degradation of connexin 43 by a proteasome-dependent mechanism. J Biol Chem 279:27219–27224.

Figueroa XF, Duling BR (2009) Gap junctions in the control of vascular function. Antioxid Redox Signal 11:251–266.

Folbergrová J, Memezawa H, Smith ML, Siesjö BK (1992) Focal and perifocal changes in tissue energy state during middle cerebral artery occlusion in normo- and hyperglycemic rats. J Cereb Blood Flow Metab 12:25–33.

Frisina ST, Mapes F, Kim S, Frisina DR, Frisina RD (2006) Characterization of hearing loss in aged type II diabetics. Heart Res 211:103–113.

Gandhi GK, Cruz NF, Ball KK, Theus SA, Dienel GA (2009a) Selective astrocytic gap junctional trafficking of molecules involved in the glycolytic pathway: impact on cellular brain imaging. J Neurochem 110:857–869.

Gandhi GK, Cruz NF, Ball KK, Dienel GA (2009b) Astrocytes are poised for lactate trafficking and release from activated brain and for supply of glucose to neurons. J Neurochem 111:522–536.

García-Espinosa MA, García-Martín ML, Cerdán S (2003) Role of glial metabolism in diabetic encephalopathy as detected by high resolution 13C NMR. NMR Biomed 16:440–449.

Giaume C, Marin P, Cordier J, Glowinski J, Premont J (1991) Adrenergic regulation of intercellular communications between cultured striatal astrocytes from the mouse. Proc Natl Acad Sci USA 88:5577–5581.

Heath DF, Rose JG (1969) The distribution of glucose and [^{14}C]glucose between erythrocytes and plasma in the rat. Biochem J 112:373–377.

Hertz L, Peng L, Lai J C (1998) Functional studies in cultured astrocytes. Methods 16:293–310.

Hink U, Li H, Mollnau H, Oelze M, Matheis E, Hartmann M, Skatchkov M, Thaiss F, Stahl RA, Warnholtz A, et al. (2001) Mechanisms underlying endothelial dysfunction in diabetes mellitus. Circ Res 88:E14–E22.

Hofer RE, Lanier WL (1991a) The effects of insulin infusion on plasma and brain glucose in hyperglycemic diabetic rats. A comparison with placebo-treated diabetic and nondiabetic rats. Anesthesiology 75:673–678.

Hofer RE, Lanier WL (1991b) Effects of insulin on blood, plasma, and brain glucose in hyperglycemic diabetic rats. Stroke 22:505–509.

Holden JE, Mori K, Dienel GA, Cruz NF, Nelson T, Sokoloff L (1991) Modeling the dependence of hexose distribution volumes in brain on plasma glucose concentration: implications for estimation of the local 2-deoxyglucose lumped constant. J Cereb Blood Flow Metab 11:171–182.

Howarth FC, Chandler NJ, Kharche S, Tellez JO, Greener ID, Yamanushi TT, Billeter R, Boyett MR, Zhang H, Dobrzynski H (2008) Effects of streptozotocin-induced diabetes on connexin43 mRNA and protein expression in ventricular muscle. Mol Cell Biochem 319:105–114.

Hoxworth JM, Xu K, Zhou Y, Lust WD, LaManna JC (1999) Cerebral metabolic profile, selective neuron loss, and survival of acute and chronic hyperglycemic rats following cardiac arrest and resuscitation. Brain Res 821:467–479.

Huber JD, VanGilder RL, Houser KA (2006) Streptozotocin-induced diabetes progressively increases blood–brain barrier permeability in specific brain regions in rats. Am J Physiol Heart Circ Physiol.291:H2660–H2668.

Inoguchi T, Ueda F, Umeda F, Yamashita T, Nawata H (1995) Inhibition of intercellular communication via gap junction in cultured aortic endothelial cells by elevated glucose and phorbol ester. Biochem Biophys Res Commun 208:492–497.

Inoguchi T, Yu HY, Imamura M, Kakimoto M, Kuroki T, Maruyama T, Nawata H (2001) Altered gap junction activity in cardiovascular tissues of diabetes. Med Electron Microsc 34:86–91.

Itoh Y, Esaki T, Shimoji K, Cook M, Law MJ, Kaufman E, Sokoloff L (2003) Dichloroacetate effects on glucose and lactate oxidation by neurons and astroglia *in vitro* and on glucose utilization by brain *in vivo*. Proc Natl Acad Sci USA 100:4879–4884.

Jacob RJ, Fan X, Evans ML, Dziura J, Sherwin RS (2002) Brain glucose levels are elevated in chronically hyperglycemic diabetic rats: no evidence for protective adaptation by the blood–brain barrier. Metabolism 51:1522–1524.

Kamal A, Biessels GJ, Urban IJ, Gispen WH (1999) Hippocampal synaptic plasticity in streptozotocin-diabetic rats: impairment of long-term potentiation and facilitation of long-term depression. Neuroscience 90:737–745.

Kamal A, Biessels GJ, Gispen WH, Ramakers GM (2006) Synaptic transmission changes in the pyramidal cells of the hippocampus in streptozotocin-induced diabetes mellitus in rats. Brain Res 1073–1074:276–280.

Kleman AM, Yuan JY, Aja S, Ronnett GV, Landree LE (2008) Physiological glucose is critical for optimized neuronal viability and AMPK responsiveness *in vitro*. J Neurosci Methods 167:292–301.

Kodl CT, Seaquist ER (2008) Cognitive dysfunction and diabetes mellitus. Endocr Rev 29:494–511.

Kowluru RA, Abbas SN (2003) Diabetes-induced mitochondrial dysfunction in the retina. Invest Ophthalmol Vis Sci 44:5327–5334.

Kreis R, Ross BD (1992) Cerebral metabolic disturbances in patients with subacute and chronic diabetes mellitus: detection with proton MR spectroscopy. Radiology 184:123–130.

Kuroki T, Inoguchi T, Umeda F, Ueda F, Nawata H (1998) High glucose induces alteration of gap junction permeability and phosphorylation of connexin-43 in cultured aortic smooth muscle cells. Diabetes 47:931–936.

Lanier WL, Hofer RE, Gallagher WJ (1996) Metabolism of glucose, glycogen, and high-energy phosphates during transient forebrain ischemia in diabetic rats: effect of insulin treatment. Anesthesiology 84:917–925.

Li AF, Roy S (2009) High glucose-induced downregulation of connexin 43 expression promotes apoptosis in microvascular endothelial cells. Invest Ophthalmol Vis Sci 50:1400–1407.

Li AF, Sato T, Haimovici R, Okamoto T (2003) High glucose alters connexin 43 expression and gap junction intercellular communication activity in retinal pericytes. Invest Ophthalmol Vis Sci 44:5376–5382.

Li ZG, Zhang W, Sima AA (2007) Alzheimer-like changes in rat models of spontaneous diabetes. Diabetes 56:1817–1824.

Lin H, Ogawa K, Imanaga I, Tribulova N (2006) Remodeling of connexin 43 in the diabetic rat heart. Mol Cell Biochem 290:69–78.

Lin H, Mitasikova M, Dlugosova K, Okruhlicova L, Imanaga I, Ogawa K, Weismann P, Tribulova N (2008) Thyroid hormones suppress epsilon-PKC signalling, down-regulate connexin-43 and increase lethal arrhythmia susceptibility in non-diabetic and diabetic rat hearts. J Physiol Pharmacol 59:271–285.

Little AA, Edwards JL, Feldman EL (2007) Diabetic neuropathies. Pract Neurol 7:82–92.

Luchsinger JA, Gustafson DR (2009) Adiposity, type 2 diabetes, and Alzheimer's disease. J Alzheimers Dis 16:693–704.

Makino A, Platoshyn O, Suarez J, Yuan JX, Dillmann WH (2008) Downregulation of connexin40 is associated with coronary endothelial cell dysfunction in streptozotocin-induced diabetic mice. Am J Physiol Cell Physiol 295:C221–C230.

Malfait M, Gomez P, van Veen TA, Parys JB, De Smedt H, Vereecke J, Himpens B (2001) Effects of hyperglycemia and protein kinase C on connexin43 expression in cultured rat retinal pigment epithelial cells. J Membr Biol 181:31–40.

Mans AM, DeJoseph MR, Davis DW, Hawkins RA (1988) Brain energy metabolism in streptozotocin-diabetes. Biochem J 249:57–62.

Manschot SM, Gispen WH, Kappelle LJ, Biessels GJ (2003) Nerve conduction velocity and evoked potential latencies in streptozotocin-diabetic rats: effects of treatment with an angiotensin converting enzyme inhibitor. Diabetes Metab Res Rev 19:469–477.

Manschot SM, Biessels GJ, Rutten GE, Kessels RC, Gispen WH, Kappelle LJ; Utrecht Diabetic Encephalopathy Study Group (2008) Peripheral and central neurologic complications in type 2 diabetes mellitus: no association in individual patients. J Neurol Sci 264:157–162.

Manthey D, Banach K, Desplantez T, Lee CG, Kozak CA, Traub O, Weingart R, Willecke K (2001) Intracellular domains of mouse connexin26 and -30 affect diffusional and electrical properties of gap junction channels. J Membr Biol 181:137–148.

McCall AL (1992) The impact of diabetes on the CNS. Diabetes 41:557–570.

McCall AL (2004) Cerebral glucose metabolism in diabetes mellitus. Eur J Pharmacol 490:147–158.

McCall AL (2005) Altered glycemia and brain – update and potential relevance to the aging brain. Neurobiol Aging 26 (Suppl. 1):70–75.

McCoy E, Sontheimer H (2010) MAPK induces AQP1 expression in astrocytes following injury. Glia 58:209–217.

Mïinea C, Kuruvilla R, Merrikh H, Eichberg J (2002) Altered arachidonic acid biosynthesis and antioxidant protection mechanisms in Schwann cells grown in elevated glucose. J Neurochem 81:1253–1262.

Mooradian AD (1997) Pathophysiology of central nervous system complications in diabetes mellitus. Clin Neurosci 4:322–326.

Moyer Jr JR, Brown TH (1998) Patch-clamp techniques applied to brain slices. In Neuromethods Vol. 35: Patch-clamp Analysis: Advanced Techniques (Walz W, Boulton AA, Baker GB, eds), pp. 135–193, Humana Press, Totowa, NJ.

O'Brien J, Kla KM, Hopkins IB, Malecki EA, McKenna MC (2007) Kinetic parameters and lactate dehydrogenase isozyme activities support possible lactate utilization by neurons. Neurochem Res 32:597–607.

Oku H, Kodama T, Sakagami K, Puro DG (2001) Diabetes-induced disruption of gap junction pathways within the retinal microvasculature. Invest Ophthalmol Vis Sci 42:1915–1920.

Özcan U, Cao Q, Yilmaz E, Lee AH, Iwakoshi NN, Ozdelen E, Tuncman G, Görgün C, Glimcher LH, Hotamisligil GS (2004) Endoplasmic reticulum stress links obesity, insulin action, and type 2 diabetes. Science 306:457–461.

Özcan U, Yilmaz E, Ozcan L, Furuhashi M, Vaillancourt E, Smith RO, Gorgun CZ, Hotamisligil GS (2006) Chemical chaperones reduce ER stress and restore glucose homeostasis in a mouse model of type 2 diabetes. Science 313:1137–1140.

Pellerin L, Magistretti PJ (1994) Glutamate uptake into astrocytes stimulates aerobic glycolysis: a mechanism coupling neuronal activity to glucose utilization. Proc Natl Acad Sci USA 91:10625–10629.

Pellerin L, Magistretti PJ (2005) Ampakine CX546 bolsters energetic response of astrocytes: a novel target for cognitive-enhancing drugs acting as alpha-amino-3-hydroxy-5-methyl-4-isoxazolepropionic acid (AMPA) receptor modulators. J Neurochem 92:668–677.

Peters O, Schipke CG, Philipps A, Haas B, Pannasch U, Wang LP, Benedetti B, Kingston AE, Kettenmann H (2009) Astrocyte function is modified by Alzheimer's disease-like pathology in aged mice. J Alzheimer's Dis 18:177–189.

Puchowicz MA, Xu K, Magness D, Miller C, Lust WD, Kern TS, LaManna JC (2004) Comparison of glucose influx and blood flow in retina and brain of diabetic rats. J Cereb Blood Flow Metab 24:449–457.

Roberts RO, Geda YE, Knopman DS, Christianson TJ, Pankratz VS, Boeve BF, Vella A, Rocca WA, Petersen RC (2008) Association of duration and severity of diabetes mellitus with mild cognitive impairment. Arch Neurol 65:1066–1073.

Romanovsky D, Cruz NF, Dienel GA, Dobretsov M (2006) Mechanical hyperalgesia correlates with insulin deficiency in normoglycemic streptozotocin-treated rats. Neurobiol Dis 24:384–394.

Rubini R, Biasiolo F, Fogarolo F, Magnavita V, Martini A, Fiori MG (1992) Brainstem auditory evoked potentials in rats with streptozotocin-induced diabetes. Diabetes Res Clin Pract 16:19–25.

Ruderman NB, Ross PS, Berger M, Goodman MN (1974) Regulation of glucose and ketone-body metabolism in brain of anaesthetized rats. Biochem J 138:1–10.

Sato T, Haimovici R, Kao R, Li AF, Roy S. (2002) Downregulation of connexin 43 expression by high glucose reduces gap junction activity in microvascular endothelial cells. Diabetes 51:1565–1571.

Shram NF, Netchiporouk LI, Martelet C, Jaffrezic-Renault N, Cespuglio R (1997) Brain glucose: voltammetric determination in normal and hyperglycaemic rats using a glucose microsensor. Neuroreport 8:1109–1112.

Sima AA, Kamiya H, Li ZG (2004) Insulin, C-peptide, hyperglycemia, and central nervous system complications in diabetes. Eur J Pharmacol 490:187–197.

Sonnen JA, Larson EB, Brickell K, Crane PK, Woltjer R, Montine TJ, Craft S (2009) Different patterns of cerebral injury in dementia with or without diabetes. Arch Neurol 66:315–322.

Sorg O, Magistretti PJ (1991) Characterization of the glycogenolysis elicited by vasoactive intestinal peptide, noradrenaline and adenosine in primary cultures of mouse cerebral cortical astrocytes. Brain Res 563:227–233.

Speizer L., Haugland R. and Kutchai H (1985) Asymmetric transport of a fluorescent glucose analogue by human erythrocytes. Biochim Biophys Acta 815:75–84.

Stalmans P, Himpens B (1997) Effect of increasing glucose concentrations and protein phosphorylation on intercellular communication in cultured rat retinal pigment epithelial cells. Invest Ophthalmol Vis Sci 38:1598–1609.

Takahashi S, Driscoll BF, Law MJ, Sokoloff L (1995) Role of sodium and potassium ions in regulation of glucose metabolism in cultured astroglia. Proc Natl Acad Sci USA 92:4616–4620.

Tampo Y, Kotamraju S, Chitambar CR, Kalivendi SV, Keszler A, Joseph J, Kalyanaraman B (2003) Oxidative stress-induced iron signaling is responsible for peroxide-dependent oxidation of dichlorodihydrofluorescein in endothelial cells: role of transferrin receptor-dependent iron uptake in apoptosis. Circ Res 92:56–63.

Tang J, Zhu XW, Lust WD, Kern TS (2000) Retina accumulates more glucose than does the embryologically similar cerebral cortex in diabetic rats. Diabetologia 43:1417–1423.

Tay HL, Ray N, Ohri R, Frootko NJ (1995) Diabetes mellitus and hearing loss. Clin Otolaryngol Allied Sci 20:130–134.

van der Graaf M, Janssen SW, van Asten JJ, Hermus AR, Sweep CG, Pikkemaat JA, Martens GJ, Heerschap A (2004) Metabolic profile of the hippocampus of Zucker diabetic fatty rats assessed by *in vivo* 1H magnetic resonance spectroscopy. NMR Biomed 17:405–410.

Vaughan N, James K, McDermott D, Griest S, Fausti S (2006) A 5-year prospective study of diabetes and hearing loss in a veteran population. Otol Neurotol 27:37–43.

Vaughan N, James K, McDermott D, Griest S, Fausti S (2007) Auditory brainstem response differences in diabetic and non-diabetic veterans. J Am Acad Audiol 18:863–871.

Wagner 4th SR, Lanier WL (1994) Metabolism of glucose, glycogen, and high-energy phosphates during complete cerebral ischemia. A comparison of normoglycemic, chronically hyperglycemic diabetic, and acutely hyperglycemic nondiabetic rats. Anesthesiology 81:1516–1526.

Welch WJ, Brown CR (1996) Influence of molecular and chemical chaperones on protein folding. Cell Stress Chaperones 1:109–115.

Wolff JR, Stuke K, Missler M, Tytko H, Schwarz P, Rohlmann A, Chao TI (1998) Autocellular coupling by gap junctions in cultured astrocytes: a new view on cellular autoregulation during process formation. Glia 24:121–140.

Ye ZC, Ransom BR, Sontheimer H (2001) (1*R*,3*S*)-1-Aminocyclopentane-1,3-dicarboxylic acid (RS-ACPD) reduces intracellular glutamate levels in astrocytes. J Neurochem 79:756–766.

Ye ZC, Wyeth MS, Baltan-Tekkok S, Ransom BR (2003) Functional hemichannels in astrocytes: a novel mechanism of glutamate release. J Neurosci 23:3588–3596.

Ye ZC, Oberheim N, Kettenmann H, Ransom BR (2009) Pharmacological 'cross-inhibition' of connexin hemichannels and swelling activated anion channels. Glia 57:258–269.

Yu N, Martin JL, Stella N, Magistretti PJ (1993) Arachidonic acid stimulates glucose uptake in cerebral cortical astrocytes. Proc Natl Acad Sci USA 90:4042–4046.

Received 19 October 2009/3 January 2010; accepted 5 January 2010

Published as Immediate Publication 5 January 2010, doi 10.1042/AN20090048